

1 Estimating climate-driven phenology shifts and survey 2 availability using fishery-dependent data

3
4 Maxime Olmos^{1,2,3*}, James Ianelli³, Lorenzo Ciannelli², Ingrid Spies³, Carey R. McGilliard^{3*},
5 James T. Thorson^{3*}

6 ¹*Present address:* DECOD (Ecosystem Dynamics and Sustainability), IFREMER, INRAE, Institut
7 Agro, ZI Pointe du Diable, Plouzane F-29280, France

8 ²College of Earth, Ocean and Atmospheric Sciences, Oregon State University, Corvallis, OR
9 97331, USA

22 ³Alaska Fisheries Science Center, National Marine Fisheries Service, National Oceanic and
23 Atmospheric Administration, 7600 Sand Point Way NE, Seattle, WA 98115, USA

24 * Corresponding authors

25 maxime.olmos@ifremer.fr

26 carey.mcgiiliard@noaa.gov

27 james.thorson@noaa.gov

28 29 HIGHLIGHTS

- 30 • Climate-driven phenology shifts has been inferred using seasonal spatio-temporal models
31 and fishery-dependent data
- 32
33 • Spawning movement phenology occurs earlier during warm years than cold years
34
- 35 • Spatial distribution is more constrained, and biomass is lower during cold years than
36 warm years
37
- 38 • Fish were more available to the summer survey during warm years than cold years
39 because of earlier spawning migration during warm years
40
- 41 • Phenology differed by sex with males staying longer on the spawning grounds than
42 females.
43
- 44 • Fishery-dependent data can be used to compute a catchability covariate within the
45 yellowfin stock assessment.
46
47
48
49

50 **ABSTRACT**

51 Environmental changes are predicted to impact fish ecology; specifically, the phenology of
52 spawning and larval settlement, resulting adult and larval movement, and ultimately seasonal
53 habitat utilization. Hence, warm or cold environmental conditions may cause early or late seasonal
54 movement among habitats. However, resource surveys are typically designed to occur at
55 approximately the same time each year, and this mismatch in timing between survey sampling and
56 fish movement can cause a different proportion of population biomass to be available to the survey
57 in different years. In this study, we demonstrate an application to minimize such impacts using
58 yellowfin sole (*Limanda aspera*) in the eastern Bering Sea as a case study. We employed fishery-
59 dependent catch-and-effort (also called catch per unit effort (CPUE)) data collected by observers
60 on commercial vessels, which covered the months of March-October (whereas survey data were
61 limited to June-August). We built a seasonal spatio-temporal model so that seasonal distribution
62 could be used to better explain summer survey availability and movement timing as impacted by
63 interannual temperature changes. Our results highlight (i) spawning movement phenology occurs
64 earlier during warm years than cold years, (ii) spatial distribution is more constrained and biomass
65 is lower during cold years than warm years, (iii) fish were more available to the summer survey
66 during warm years than cold years, and (iv) phenology differed by sex with males staying longer
67 on the spawning grounds than females. Finally, we computed an overlap index between the survey
68 area and fishery CPUE data to be used as a catchability covariate within the yellowfin sole stock
69 assessment. This index confirmed the changes in relative availability of this species by year as
70 presently used in the assessment.

71 **Keywords:** movement phenology, climate-driven phenology shifts, seasonal spatiotemporal
72 model, fishery-dependent data, spatial availability, catchability, yellowfin sole.

73

74

I. INTRODUCTION

75

76

77

78

79

80

81

82

83

Rapid environmental changes to fish habitat present several major challenges to fisheries ecology and management. In response to a changing climate, marine organisms can adapt to the new conditions within their current geographical range, can track their climatic niches in time and/or in space or can become locally extinct (García Molinos et al., 2016). This can lead to changes in the ecosystem structure and functioning across space and time. To track their niche in space and time, marine organisms have to adapt by changing the seasonal timing of many biological processes (termed “phenology”), including the timing of spawning and larval settlement, resulting adult and larval movement, and ultimately seasonal habitat utilization (Rogers and Dougherty, 2019).

84

85

86

87

88

89

90

91

92

93

94

95

96

97

98

99

100

101

102

103

104

105

106

107

108

109

110

111

112

113

114

115

116

117

118

Accounting for such spatial and temporal aspects of climate responses can be critical to successfully manage fisheries. Previous studies have shown that spawning phenology, particularly spawning migration phenology, is sensitive to temperature in fish species conducting ontogenetic migration (McQueen and Marshall, 2017; Sims et al., 2004). For example, climate-induced changes in spawning phenology has been shown for striped bass (*Morone saxatilis*) (Peer and Miller 2014) in Chesapeake Bay, which led to higher than anticipated fishing mortality on spawning fish during cold years. Resource surveys for use in stock assessments are typically designed to occur at approximately the same time each year (NRC, 2000). However, warm or cold temperature conditions may cause early or late movement (Asch, 2015) into or out of the survey area causing differential “availability” of the resource (Staudinger et al., 2019). The ability to detect such climate impacts requires models that can use additional data and handle seasonal, interannual, and spatial processes, and these are rare (Sydeman et al., 2015; Thorson et al., 2020). Some movement phenology studies have focused on anadromous fish because of easier access to their spawning grounds and juvenile habitats in rivers (Kovach et al., 2015; Otero et al., 2014). For oceanic conditions, habitat and seasonal coverages are challenging. Fishery-dependent data can expand our “snapshot” survey data and improve understanding of essential fish habitat (Dambrine et al., 2021; Murray et al., 2013). The expanded seasonal and spatial coverage can then be useful to explore biological processes such as spawning within a large spatial domain (Neidetcher et al., 2014). But fishery-dependent data present some limits (Maunder et al., 2006) because those data might confound changes in fishing behavior with trends in abundance. Considering fishing behavior is then important to avoid biased estimates of biomass and distribution. Nevertheless, fishery-dependent have been widely used to provide inside about fishery ecosystems functioning (Pauly et al., 1998) and to characterize seasonal distribution and habitat use (Kneebone et al., 2020). Indeed, previous studies highlighted that fishery-dependent and independent data might provide very similar patterns in term of fish spatio-temporal distributions (Pennino et al., 2016). With respect to spatio-temporal models, previous authors have included seasonal variation in isolation (Grieve et al., 2017; Thorson et al., 2016) or included both changes in spatial distribution among years and among seasons (Akia et al., 2021; Bourdaud et al., 2017; Kai et al., 2017; Kanamori et al., 2019). In particular, (Thorson et al., 2020) built seasonally explicit spatiotemporal models that included annual and seasonal variation in spatial distribution and density to identify interannual changes in phenology. Those models can be useful to identify climate-driven shifts in the seasonal timing of fish movement and ecosystem productivity but are expensive in terms of parametrization, and computation time. Spatio-temporal models that account for seasons when fit to fishery data may suffer from unbalanced designs and a lack of parsimony. In this study, we resolve this problem by an alternative approach accounting for seasonality

119 implicitly, using spatially varying catchability to represent seasonality. This allows us to explore
120 migration timing and how interannual temperature changes impact seasonal migrations.

121
122 We implemented this approach on yellowfin sole (*Limanda aspera*) from the eastern Bering
123 Sea (EBS). This stock represents the largest flatfish fishery in the world by landed weight (Spies
124 et al., 2019). Adults exhibit a benthic lifestyle and occupy separate spawning areas (in summer)
125 and feeding areas (in late summer) on the eastern Bering Sea shelf. From over-wintering grounds
126 near the shelf margins, adults begin a migration onto the inner shelf in spring each year for
127 spawning and feeding (Nichol, 1995; Wakabayashi, 1989; Wilderbuer et al., 1992) (Fig.1). The
128 directed fishery historically occurs from winter through autumn, and NMFS research surveys take
129 place during the summer months (Wilderbuer et al., 1992). The availability of this stock has been
130 shown to vary within the survey area (Nichol, 1998; Nichol et al., 2019) due to spawning
131 migrations. Presently, the stock assessment model used for setting catch advice includes a
132 temperature coefficient that impacts the availability of the stock to the survey gear (Wilderbuer et
133 al., 2019).

134 As with other flatfish stocks where males remain on the spawning grounds longer than
135 females (Arnold and Metcalfe, 1996; Hirose and Minami, 2007; Rijnsdorp, 1989; Solmundsson et
136 al., 2003), Nichol et al., (2019) also showed that male yellowfin sole remained on the spawning
137 grounds longer than females and highlighted positive correlations between the proportion of
138 females relative to male and annual estimated survey biomass. However, all those conclusions rely
139 on data collected from scientific surveys designed to occur at the same time each year within the
140 same restrained spatial domain, which precludes our understanding of changes in timing of
141 spawning migration. No seasonal or interannual processes have been inferred to better understand
142 the impact of interannual temperature changes on yellowfin sole movement phenology. In this
143 paper, using fishery-dependent catch per unit effort data (CPUE), we propose to extend these
144 previous findings (Nichol et al., 2019) by inferring seasonal movement and relationships between
145 movement and interannual temperature changes. Because spatially explicit fishery CPUE data are
146 available throughout multiple seasons and years, it can be used to build a model on a sub-seasonal
147 interval to capture seasonal movement within a wide spatial domain. We developed a model which
148 accounts for seasonality implicitly and explored how migration timing and interannual temperature
149 changes can impact the spatiotemporal distribution of CPUE data. To this end, we estimated
150 spatially varying catchability coefficients linking density, seasons, and interannual temperature
151 changes. We specifically define early (March 19-May 21), intermediate (May 22-July 30), and late
152 (August 1-September 24) fishing seasons for yellowfin sole. These seasons include 33.2%, 32.7%,
153 32.6% respectively of the total fishery landings from 2001 and 2019. This study's period (March
154 19-September 24) corresponds to high fishing effort that brackets spawning timing and migration
155 of yellowfin sole in the Bering Sea and includes the fishery-independent survey timing occurring
156 during the intermediate season.

157 We address four key questions:

158 **[Q1] Does the timing of migration and progression of spawning impact the fishery CPUE**
159 **and is the progression of spawning dependent on temperature changes in the EBS?**

160 During warm years, we expect migrations to start earlier, with high CPUE in the middle shelf
161 during the early season, and then again in the middle and outer shelf during the late season when
162 back migration is more progressed (Fig. 2, second row). Inversely, during cold years, we expect

163 migration to be delayed with high CPUE in the inner shelf and in the middle shelf during the
164 intermediate and late season respectively, when back migration to wintering areas is delayed (Fig.
165 2, second row).

166 **[Q2] Does fish availability to survey change between warm and cold years?**

167 During warm years, because migrations are more progressed, we expect substantial overlap
168 between survey area and fisheries CPUE during the intermediate season (i.e. during the survey
169 timing). By contrast during cold years, fish are expected to be in shallower water during the
170 intermediate season and not available to the survey, so we expect lower overlap between survey
171 area and fisheries CPUE during the intermediate season, while we expect a strong overlap during
172 the late season when fish starts leaving spawning grounds to wintering areas (Fig. 2).

173 **[Q3] Does phenology, that is the timing of spawning migration, change with sex?**

174 We expect male yellowfin sole remain on the spawning grounds longer than females, because
175 females appear to migrate out of the spawning areas earlier than males, based on analyses from
176 survey data (Nichol et al., 2019).

177 **[Q4] Can we use fishery CPUE to account for change in availability to the survey to improve
178 the yellowfin stock assessment?**

179 The yellowfin stock assessment (Spies et al., 2019) includes the survey mean bottom temperature
180 and survey timing across stations as covariates affecting survey catchability. We evaluate how an
181 “overlap index” computed from seasonal fishery CPUE (derived from [Q2]) might improve the
182 assessment of yellowfin sole in the eastern Bering Sea.

183

184

185 **II. MATERIALS AND METHODS**

186 In this section, we will first present the spatiotemporal models in a general way so that it can be
187 applied to other cases of study, then the data specific to our case study, and then the specific
188 methodologies to address the questions posed above.

189 **II.1. Spatio-temporal model accounting implicitly for seasonal variations**

190

191 We developed spatiotemporal models which estimate the expected fisheries CPUE $b(s_i, t_i)$ (in
192 biomass per tow duration) for each sample i , occurring at location s_i and year t_i .

193

194 To define the spatial resolution of the model, we adopted the SPDE (Stochastic Partial Differential
195 Equation) spatial framework which represents continuous Gaussian fields as a discrete Gaussian
196 Markov random field (Lindgren, 2012). The number of knots determines the spatial resolution of
197 the model (and is specified by the user as a trade-off between the accuracy of the Gaussian Markov
198 random fields representation and computational cost). We used a k-means algorithm to identify
199 the location of knots to minimize the total distance between the location of knots and extrapolation-
200 grid cells (Fig. S1). The SPDE approximation involves generating a triangulated mesh that has a
201 vertex of a triangle at each knot (here we used the package *R-INLA* (Lindgren, 2012)). Then spatial
202 variables at location s , are interpolated from knots to extrapolation grid using this triangulated

203 mesh (Fig. S1) (Grüss et al., 2020). Concerning the temporal resolution of the model, year t_i is
 204 defined as an integer $\{2001, 2002, \dots, 2019\}$. We calculate $b(s_i, t_i)$ using a Generalized Linear
 205 Mixed Model (GLMM) while including random effects to describe additional variability from
 206 covariates not included in the process error terms (spatial and spatiotemporal variations, more
 207 details below in equation (1)). We specifically define a linear predictor that is then transformed
 208 via an inverse-link function. In the following we used a log-link function, so that all effects are
 209 additive in their impact on predicted fisheries log-CPUE, which also simplifies interpretation of
 210 covariate effects.

211 The model is a log-linked linear predictor as follows:

$$212 \log [b(s_i, t_i)] = \beta(t_i) + \sum_{k=1}^{n_k} ((\lambda(k) + \varphi(s_i, k)) q(i, k)) + \omega(s_i) + \varepsilon(s_i, t_i), \quad (1)$$

213 where $\beta(t_i)$ is the intercept for year t_i , $\omega(s_i)$ and $\varepsilon(s_i, t_i)$ represent, respectively, spatial, and
 214 spatiotemporal variation in fishery CPUE; and $q(i, k)$ is an element of matrix q composed of n_k
 215 measured catchability covariates that explain variation in catchability, $\lambda(k)$ is the estimated impact
 216 of catchability covariates for this linear predictor, $\varphi(s_i, k)$ is zero-centered spatial variation in that
 217 slope term. The model was designed to predict fishery CPUE as a function of temporal variation,
 218 spatial variation, and spatiotemporal variation effects, as well as catchability covariates. It accounts
 219 for these spatio-temporal dynamics as follows:

- 221 1. Spatial variation: the spatial variation terms, $\omega(s)$, in Equation (1) represent unmeasured
 222 spatial variation in the linear predictor that is stable over time;
- 223 2. Spatio-temporal variation: the spatiotemporal variation terms $\varepsilon(s,t)$, represent unmeasured
 224 spatial variations in the linear predictors that changes between years;
- 225 3. Temperature-mediated drivers represented as catchability: $\varphi(s, k)$ in Equation (1)
 226 encompasses the spatially varying effect of covariates on fisheries CPUE. A part of the
 227 spatial variation is then attributed to catchability covariates. For each catchability
 228 covariate (indexed by k) tested, we implemented corner constraints only for the linear
 229 effect $\lambda(k)$, and not for the spatially varying effect $\varphi(s_i, k)$.

230
 231 These spatial and spatio-temporal terms can be modelled as random effects following a
 232 multivariate normal distribution (Gaussian random fields):

$$233 \begin{aligned} \boldsymbol{\omega} &\sim MVN(\mathbf{0}, \sigma_{\omega}^2 \mathbf{R}_{\omega}) \\ \boldsymbol{\varepsilon}(t) &\sim MVN(0, \sigma_{\varepsilon}^2 \mathbf{R}_{\varepsilon}) \\ \boldsymbol{\varphi}(k) &\sim MVN(0, \sigma_{\varphi}^2 \mathbf{R}_{\varphi}) \end{aligned} \quad (2)$$

234 where σ_{ω}^2 is the estimated pointwise variances of the spatial variation in CPUE; σ_{ε}^2 is the estimated
 235 pointwise variances of the spatio-temporal variation in CPUE; σ_{φ}^2 is the estimated pointwise
 236 variances of the spatial effect for each covariate k ; $\mathbf{R}(s_1, s_2)$ is the correlation between location s_1
 237 and location s_2 for spatial and spatiotemporal terms and is approximated as following a Matern
 238 function:

$$239 \mathbf{R}(s_1, s_2) = \frac{1}{2^{\nu-1} \Gamma(\nu)} \times (\kappa |(s_1 - s_2) \mathbf{H}|)^{\nu} \times K_{\nu}(\kappa |(s_1 - s_2) \mathbf{H}|) \quad (3)$$

240 where \mathbf{H} is a two-dimensional linear transformation representing geometric anisotropy, ν is the
241 Matern smoothness (fixed at 1.0), and κ governs the decorrelation distance.

242 Finally, in this study, we analyzed fisheries dependent data, in particular those CPUE data that did
243 not include zeros, and we assumed CPUE by location to be lognormally distributed. Code for
244 model M3 is available online on Github (https://github.com/MaxOlmos/Flat_fish_2021).

245 II. 2. Data

246 *Fishery-dependent catch-and-effort (CPUE)*

247 We used catch (biomass in kg) and effort (tow duration) data collected by observers on Bering
248 Sea-Aleutian Islands commercial bottom trawl vessels from 2001 to 2019 between March 19-
249 September 24. For each commercial catch, observers record geographical position (longitude and
250 latitude) and total catch of yellowfin sole, extrapolated from a sample. Sample locations are
251 defined as the centroid of one of 105 polygons defined by the Alaska Department of Fish and
252 Game (called ADFG cells, one degree of longitude by half degree latitude), where these cells
253 encompass the spatial domain of yellowfin sole fishery in the eastern Bering Sea (Suppl. Mat. Fig.
254 S2, S3). We aggregated all observed sets within a given year, season (early/intermediate/late), and
255 ADFG spatial cell to a single observation. We aggregated from observed sets to unique year-cell-
256 season combinations in two ways:

- 257 1. Average ratio: We present results based on this method by calculating the ratio of catch and
258 effort for each observed set, and then averaged across these. This “average ratio” has also
259 been done in model-based analyses and allows to correct for effects of changes in the
260 distribution of fishing fleets and activity (Walters, 2003; Walters and Hilborn, 2005)
- 261 2. Ratio estimator: As a sensitivity analysis, we separately summed the catch and effort for all
262 observed sets, and then taking the ratio of these sums (Swain and Wade, 2003). This is
263 conceptually similar to “ratio estimators” (Myers and Worm, 2003);

264 In practice, we found that results were not highly sensitive to the choice of aggregation method
265 (Suppl. Mat. Fig. S5, S6) so the spatio-temporal model was fit to these aggregated data (using the
266 average ratio method). Also, this aggregating process is designed to mitigate the potential bias
267 arising from preferential sampling (Alglave et al., 2022; Conn et al., 2017), by ensuring that areas
268 with a disproportionately higher CPUE of observed sets are still aggregated to a single fitted
269 observation. As a preliminary check and as suggested by Alglave et al. (2022), we explored the
270 relationship between sampling intensity and biomass to diagnose any potential strong preferential
271 sampling. Our results suggested that preferential sampling is low (Suppl. Mat. Fig. S4), so we did
272 not account for any preferential sampling in our model.

273 *Catchability covariates*

274 We sought to understand how the spatiotemporal distribution of CPUE changed depending on
275 warm or cold temperature years. Thorson, (2019a) has assessed the impact of temperature and cold
276 pool on yellowfin sole. But this study relied on survey data that are only defined for the
277 intermediate season. Unfortunately, no temperature associated with fishery CPUE samples are
278 available. So, based on Nichol et al. (2019) and the time variation in cold pool extent (Suppl. Mat.
279 Fig. S7, *akgfmmaps* package (<https://github.com/afsc-gap-products>) we approximated interannual
280 temperature changes in the Bering Sea using temperature as a discrete variable with two levels:
281 nine cold years (2006-2013, 2017) and ten warm years (2001-2005, 2014-2016, 2018, and 2019).

282 We encourage future work using other covariates to approximate interannual temperature changes
283 in the Bering Sea such as temperature (continuous variable, yearly or seasonally defined) and cold
284 pool extent.

285 The *season* covariate is discrete with three levels which were based on the migration ecology of
286 yellowfin sole (Nichol, 1998; Spies et al., 2019; Wilderbuer et al., 1992): early (March 19-May
287 21), intermediate (May 22-July 30), and late seasons (August 1-September 24), where these
288 seasons include 33.2% , 32.7% and 32.6%, respectively of the total fishery landings between 2001
289 and 2019, and the survey occurs during the intermediate season (between 2001 and 2019, more
290 than 99.9% of the survey tows occurs during the intermediate season).

291 To implicitly estimate changes in movement phenology depending on temperature changes in the
292 EBS we considered the combined effect of *interannual temperature changes* and *season* on fishery
293 CPUE data.

294 Different models for the spatiotemporal variation of fishery CPUE were tested (Table 1). In the
295 reference model M3, we inferred whether the timing of migration (i.e., season) changes with
296 different environmental conditions (i.e., for years with warm or cold years). Three models of lower
297 complexity were also considered (M0, M1, M2, Table 1) to test if accounting implicitly for
298 seasonal movement (i.e., season and temperature effects) better explains the spatiotemporal
299 variations in fishery CPUE data. We used Akaike’s Information Criterion (AIC) for model
300 selection as a measure of model parsimony to identify the level of complexity that likely minimizes
301 the combination of bias (Akaike, 1974).

302 *Male and female data*

303 Fisheries CPUE were apportioned into male and female categories using female proportion data
304 from observer data. For some locations, female proportions do not exist (17% of the locations). In
305 this case we attributed to this location the value of the closest neighbor for a given year and a given
306 combination of covariates (i.e., all combinations of levels constituting the *seasons* covariates)
307 (Suppl. Mat. Fig.S8).

308

309 **II.3. Estimation and model fitting**

310 Parameters are estimated using release 3.8.2 of the Vector Autoregressive Spatio-Temporal
311 (VAST) package (Thorson, 2019), which is publicly available online ([https://github.com/James-](https://github.com/James-Thorson/VAST)
312 [Thorson/VAST](https://github.com/James-Thorson/VAST)) and runs within the R statistical environment (R Core Team, 2017). Spatial terms
313 were estimated using the SPDE approximation (Lindgren et al. 2011), such that we estimate the
314 value of each spatial variable at a set of knots.

315 The marginal log likelihood was computed using the Laplace approximation implemented by the
316 R package ‘TMB’ (Kristensen et al., 2016) through an approximation of the integral across all
317 random effects. Finally, VAST employs the generalized delta method implemented in TMB to
318 calculate the standard errors of all the fixed and random effects, as well as the standard errors of
319 the derived quantities (Kass & Steffey 1989). In some cases, we also calculated standard errors
320 (SEs) for entire vectors of output (e.g., $se(\varphi(s, k))$ for the spatially varying term φ). In these
321 cases, we extracted the joint precision matrix (e.g., matrix of 2nd derivatives) of fixed and random

322 effects evaluated at their maximum likelihood estimates and conditional upon the data. We then
 323 generated 250 samples from this joint precision matrix, recompute all quantities for each sample,
 324 and then calculate the standard error as the standard deviation of these samples. This
 325 approximation had lower accuracy than the generalized delta method but is computationally
 326 efficient when calculating standard errors for quantities calculated as a nonstandard function of
 327 parameters.

328 **II.4. Model validation and evaluation**

331 We assessed model convergence by checking that the gradient of the marginal log-likelihood is
 332 less than 0.0001 for all fixed effects, and that the Hessian matrix of second derivatives of the
 333 negative log-likelihood is positive definite. We checked model residuals and validated the model
 334 using the DHARMA framework (Hartig, 2022) within VAST by computing QQ-plot residuals
 335 (Suppl. Mat. Fig. S10), plotting how residuals vary with magnitude of the predictions (Suppl. Mat.
 336 Fig. S10), and spatial map of quantile residuals (Suppl. Mat. Fig. S11). None of our diagnostics
 337 highlight any strong patterns in residuals and does not indicate any strong inconsistencies between
 338 the models and the data.

339 Model M3, which accounts for changes in movement phenology in response to interannual
 340 temperature changes has the lowest AIC value so appears to be the best descriptor to represent
 341 spatiotemporal variations in CPUE and was therefore retained in the subsequent analyses (Table
 342 1).

343 **II.5. Derived quantities and model specifications**

345 Here we describe the methodology used to find evidence in support of each of our fundamental
 346 questions, using results from fitting the model (Eq. 1, model M3) to the data, as described above.

347 **[Q1] Does the timing of migration and progression of spawning impact the fishery CPUE**
 348 **and is the progression of spawning dependent on interannual temperature changes in the**
 349 **EBS?**

350 We compared spatial distribution of fishery CPUE between cold and warm years. We first
 351 calculated the average predicted biomass CPUE for each season (u) in warm vs. cold years $v(t)$:

$$b(s, t, u) \equiv b(s, t) \times \varphi(s, k_{u, v(t)}) \quad (4)$$

352

$$b(s, u, v^*) = \frac{\sum_{t=1}^{n_t} I(v(t) = v^*) b(s, t, u)}{\sum_{t=1}^{n_t} I(v(t) = v^*)} \quad (5)$$

353 where $k_{u, v}$ is the covariate associated with season u and temperature v , $v(t)$ is the temperature for
 354 each year t , and $I(v(t) = v^*)$ is an indicator function that equals 1 when year t is associated with
 355 temperature v^* and 0 otherwise. So, $b(s, t, u)$ is the predicted fishery CPUE for each knot location
 356 s , in year t within season u , and $b(s, u, v^*)$ is the average fishery CPUE in season u for all years
 357 with temperature v . Then, for a given season and a given temperature, we generated and compared

358 cumulative maps of biomass ($\text{kg}\cdot\text{min}^{-1}$) by identifying the areas that encompassed the top 95th
359 percentile of total biomass across the modeled spatial domain.

360 Additionally, we assessed the significance of the spatial effect $\varphi_{u,v,s}$ for each location s , season u ,
361 and temperature v , by computing a two-sided Wald test of significance. We computed the p-value
362 assuming that the ratio $\frac{\varphi(s,k_{u,v})^2}{se(\varphi(s,k_{u,v}))^2}$ follows a Chi-squared distribution with one degree of freedom
363 (Wald Chi-Squared test). We consider the effect significant if p-value <0.05 .

364 **[Q2] Does fish availability to survey change between warm and cold years?**

365 We investigated how the spatial distribution of fisheries CPUE overlap with the survey area
366 depending on seasons and temperature. We computed an overlap index $OI(t, u)$ for each year t ,
367 each season u and each temperature $v(t)$. This overlap index $OI(t, u)$ is defined by calculating the
368 predicted fisheries biomass for all locations in the survey area ($s \in A_{Tot}$), and the predicted
369 biomass in the entire fished area ($s \in A_{EBS}$), and then calculating their ratio:

$$OI(t, u) = \frac{\sum_{s \in A_{Tot}} b(s, t) \times \varphi(s, k_{u,v(t)})}{\sum_{s \in A_{EBS}} b(s, t) \times \varphi(s, k_{u,v(t)})} \quad (6)$$

370

371 Because the predicted biomass $b(s, t, u)$ accounts for interannual variation via parameter $\beta(t)$ (see
372 Eq. 1) we also derived an overlap index from the expected spatial main effect (i.e. defined as the
373 product between $\omega(s)$ and $\varphi(s, k_{u,v})$), as a sensitivity analysis (Suppl. Mat. Fig.S9):

374

$$OI_{\omega}(u, v) = \frac{\sum_{s \in A_{Tot}} \omega(s) \times \varphi(s, k_{u,v})}{\sum_{s \in A_{EBS}} \omega(s) \times \varphi(s, k_{u,v})} \quad (7)$$

375 This sensitivity shows that the overlap index is not sensitive to the choice of Eqs. 6 or 7, so in the
376 following analysis we calculated it from $b(s, t)$ (Eq. 6).

377 **[Q3] Does phenology, i.e the timing of spawning migration, change with sex?**

378 We used the modelling framework defined in section II.1 (M3) to run two independent
379 spatiotemporal models, one for males and one for females. We extracted the predicted average
380 fishery CPUE, $b(s, u, v)$, in season u for all years with temperature $v(t)$, for both males and
381 females, to investigate if movement phenology changes between males and females depending on
382 temperature. We also extracted $OI(t, u)$ for both males and females to investigate if availability to
383 the survey changes with sex.

384 **[Q4] Can we use CPUE (results from [Q1], [Q2] and [Q3]) to account for change in 385 availability to the survey to improve the yellowfin stock assessment.**

386 We evaluated the overlap index relative to current covariates used to model survey “availability”
387 in the operational stock assessment used for management (Nichol et al., 2019). The yellowfin stock

388 assessment (Spies et al., 2019) includes the survey mean bottom temperature and survey timing
389 across stations as covariates on survey catchability, q :

$$q = e^{-\alpha + \beta_1 T + \beta_2 S + \beta_3 TS} \quad (8)$$

390 where T is survey mean bottom temperature, S is survey timing, and TS is the interaction of T and
391 S . The parameter α is the estimated intercept and β_1, β_2 and β_3 are the estimated coefficients of the
392 effect of temperature, survey timing and the interaction of temperature and survey timing on
393 catchability, respectively.

394 Presently, the assessment model code requires a covariate for every survey year. The 2021 base
395 accepted model was modified such that the current covariate anomaly values from 1982-2019, and
396 2021 were set to zero (no anomaly) except for the same years from the overlap index: 2001-2019.
397 Each covariate was normalized for the period where the overlap index is available. Three stock
398 assessment model (SAM) configurations were deemed reasonable to show for the evaluation:

399 SAM.1: Temperature, survey timing, and their interaction as covariates on catchability (Eq. 8).

400 SAM.2: Overlap index during the survey season, $OI(t, u = Int.)$, as a covariate on catchability
401 (Eq. 6).

402 We ran MCMC sampling from the posterior distribution using the ADNUTS R package
403 (Monnahan et al., 2019; Monnahan and Kristensen, 2018).

404

405 III. RESULTS

406 **[Q1] Does the timing of migration and progression of spawning impact the fishery CPUE**
407 **and is the progression of spawning dependent on temperature in the EBS?**

408 The model can predict the spatial distribution of fisheries CPUE for each year and each season
409 (Fig. 3, Suppl. Mat. Fig.S12). Our results highlight that CPUE is affected by the season and
410 progression of spawning migration. The model estimates a strong effect of seasons on the spatial
411 distribution of yellowfin sole CPUE (Fig.3, 4, 5). During the early season, CPUE are mostly
412 distributed across all EBS, whereas during the Intermediate season, CPUE are distributed in the
413 Inner Shelf, close to the spawning areas (Fig. 3). Finally, during the late season, CPUE are more
414 distributed across the inner and middle shelf where yellowfin soles have started their migration
415 back to the wintering areas in the outer shelf.

416

417 Additionally, our results highlight that the seasonal distribution of CPUE is dependent on
418 temperature. The spatiotemporal model estimates the effect of seasonality and temperature on
419 fisheries CPUE (Fig. 4, see Suppl. Mat. Fig. S13 for the significant effects). During the early
420 season, cold temperature conditions show elevated CPUE in a broad band of the outer and southern
421 middle domain while warm years show elevated CPUE in a small hotspot in the outer domain.
422 During the intermediate and late seasons, cold temperature conditions are associated with elevated
423 CPUE in the shallowest waters of the inner shelf (intermediate) or the middle domain (late), while
424 warm temperature conditions show less association with inner-domain CPUE (Fig. 4).

425

426 Seasonal distribution of CPUE is then different during warm and cold years (Fig. 5). The most
427 significant differences appear during the intermediate seasons, where yellowfin soles are
428 concentrated in the shallowest water in the inner shelf close to the spawning areas during cold
429 years, while they are less constrained and distributed in the middle shelf during warm years.

430 Collectively, our results show that spawning movement phenology is more progressed during
431 warm years than cold years. Specifically, biomass hotspots are confined to shallow waters during
432 the Intermediate season (and to a lesser degree the Late season) during cold compared with warm
433 years (Fig. 5, see middle and right panels).

434

435 **[Q2] Does fish availability to survey change between warm and cold years?**

436 Our results highlight that movement phenology in relation to interannual temperature changes in
437 the EBS affects availability of these species to the survey. During the intermediate season (which
438 corresponds to the survey season), the spatial distribution of fisheries CPUE is significantly
439 different between cold and warm years (Fig. 5). During cold years, CPUE are in the shallowest
440 water of the inner shelf close the spawning areas, mostly outside of the survey area, whereas during
441 the warm years, CPUE are found in both middle and inner shelf within the survey area.

442 Our result also suggest that yellowfin sole are more available to the survey during warm years than
443 in cold years (Fig. 6). Interannual temperature changes in the EBS impact the overlap between
444 fisheries CPUE and the survey grid, the strongest difference between warm and cold years
445 occurring during the Intermediate season (i.e., the survey season). During the survey season, warm
446 years are associated with high overlap values (~ 0.73 on average) whereas cold years are associated
447 with lower overlap (~ 0.68 in average). Finally, during late season, Fig. 6 also shows that overlap
448 is stronger during cold years suggesting that yellowfin sole has migrated back to the middle/outer
449 shelf from the inner shelf.

450 **[Q3] Does phenology, that is the timing of spawning migration, change with sex?**

451 In terms of total biomass, female biomass is larger than male biomass across the time-series (except
452 in 2013, Suppl. Mat Fig. S14). Both males and females present a seasonal pattern in their spawning
453 migration. (Fig. 7). Our results also highlight some differences. During the intermediate season,
454 males are concentrated in the spawning grounds, so very few males are available to the survey,
455 whereas females are more distributed across the inner and middle shelf, so more available to the
456 survey than males (Fig. 7). Overlap with the survey area is more important for females than males
457 for all seasons (Fig. 8), males staying longer in the inner shelf that females (Fig. 7, 2nd row,
458 columns 2 and 3).

459

460 Both males and females movement phenology is impacted by temperature (Fig. 7). In particular,
461 during the intermediate seasons, fish were more aggregated in the inner shelf during cold years
462 than warm years. Also, temperature impacted the overlap index for both males and females but
463 with approximately the same magnitude. Indeed, both males and females present a higher
464 overlap index during warm than cold years, but the difference between male and female overlap
465 index does not change with warm or cold years (Fig. 8). Standard deviations are higher in cold
466 years due to temporal variability in temperatures and cold pool extend; with some years being

467 colder than other (i.e 2012, 2013 are colder than 2011, 2017, Figure S7), which could generate
468 greater variability in terms of overlap within cold years (Fig. 5 and Fig. 7).

469
470

471 **[Q4] Can we use fishery CPUE to account for change in availability to the survey to improve**
472 **the yellowfin stock assessment?**

473 We evaluated the overlap index relative to currently used covariates (mean bottom temperature,
474 survey timing, and their interaction). For model SAM.1, both main coefficients were greater than
475 zero indicating that when the temperatures were warmer and the survey start date later, the relative
476 abundance as indexed by the standard survey area covered a greater fraction of the resource (Fig.
477 9a). This also demonstrates that the coefficient of the interaction term (of temperature and timing)
478 was negative; this would reduce the value for catchability in years where waters were warm, and
479 migration was later than normal. When we applied the overlap index alone as a covariate (SAM.2),
480 the coefficient was also significantly greater than zero which is consistent with the notion that the
481 YFS resource distribution overlaps with the survey area (Fig. 9b).

482

483 **IV. DISCUSSION**

484 In this study, we inferred movement phenology and relationships between movement and
485 interannual temperature changes using spatially explicit, year-round fishery dependent CPUE data.
486 We fit a novel spatiotemporal model that included a sub-seasonal component to these data, which
487 allowed for us to infer seasonal movement patterns. Applying this model to yellowfin sole in the
488 Bering Sea as an example, our results highlight evidence for shifts in movement phenology based
489 on seasonal temperature conditions, where spawning migration occurred earlier in warm
490 conditions. We also demonstrated these climate-related shifts in movement phenology can have
491 notable impacts on interpretation of other data sources used in stock assessment modeling (e.g.,
492 survey data) and specification of catch limits. For yellowfin sole, this was demonstrated by
493 computing an index of overlap at the time of the summer survey and using this index as a
494 catchability covariate to improve the assessment. The use of a sub-seasonal spatio-temporal
495 modeling approach fit to year-round, spatially-explicit fishery dependent data could be used to
496 explore other aspects of climate-related phenology that may be occurring for many species
497 worldwide.

498 **Consequences of climate-driven shifts in phenology on harvested populations**

499 As climate change has been impacting all ecosystems on the globe (Hoegh-Guldberg and Bruno,
500 2010; Parmesan and Yohe, 2003; Poloczanska et al., 2013) climate-driven shifts in phenology are
501 an essential concern in fisheries ecology. There is a need to account for environmental changes
502 that impact the phenology of migration to provide effective management measures. First as
503 highlighted in this study, shifts in phenology impact the fishery independent survey, designed to
504 occur at approximately the same time each year and to provide annual indices of abundance for
505 stock assessments. So, any climate-driven mismatch in timing between the survey and seasonal
506 movement dynamics can cause a different proportion of population biomass to be available to the
507 survey in different years. Long-term warming of the Bering Sea is likely to cause directional shifts
508 in seasonal movement, in turn causing long-term changes in availability to surveys. Based on our

509 results, we urge stock assessment scientists to investigate if drastic changes in stock abundance
510 represent sustained population conditions, or instead signal changes in timing of ecological events,
511 such as spawning migration.

512 Secondly, ignoring climate-driven changes in phenology when managing fisheries might lead to
513 potential overharvesting or missed harvesting opportunities. Such changes in phenology might
514 strongly impact the reproductive success of some stocks. A shift in spawning migration induced
515 by changes in temperature conditions can lead fisheries to catch adults before they could spawn
516 leading to unanticipated changes in fishing mortality (Peer and Miller, 2014). For anadromous
517 fish, accounting for phenology shifts is critical because fisheries management for those species
518 rely on expected time of fish arrival in harvested areas (Mundy and Evenson, 2011). However,
519 warm conditions lead to early migration which might be mistaken as large abundance and could,
520 in turn, lead to overharvesting. Climate-driven shifts in phenology are leading to incorporation of
521 temperature conditions in defining closed areas and fishing seasons. Zacher et al. (2018)
522 highlighted how important it is to account for the differences in red king crab (*Paralithodes*
523 *camtschaticus*) distribution with temperature regime to evaluate the effectiveness of a closed area
524 to protect crab from bycatch in trawl fisheries. Crabs were aggregated within closed areas during
525 warm years and outside closed areas during cold years, and therefore more susceptible as bycatch
526 during cold years (Zacher et al., 2018). For Pacific halibut (*Hippoglossus stenolepis*), mortality
527 applied during spawning and feeding migrations might impact biomass distribution. Changing
528 environmental conditions is altering the timing of those migrations and current fishing season
529 might be too short to protect those periods. As a consequence, allowing harvesting by seasonal
530 interception fisheries too early might impact the spawning success and the stock productivity
531 (Loher, 2011).

532 **Mechanisms underlying changes in spawning movement phenology, spatial constraints and** 533 **biomass**

534 By further examining the mechanisms underlying the yellowfin sole example, we argue that our
535 study provides insight into other species whose spatial distribution phenology may be affected by
536 climate. Our study highlights how interannual temperature changes impact the timing of spawning
537 movement but also the location and biomass of fish. During warm years the yellowfin spawning
538 migration occurs earlier with a less constrained distribution (Fig. 5) and high biomass (Fig. S14).
539 Whereas during cold years, yellowfin movement occurs later, the spatial distribution is more
540 constrained in the inner shelf, and total biomass is lower than during warmer years. Those results
541 seem to be in accordance with previous studies (Bartolino et al., 2011; Nichol et al., 2019; Porter,
542 2022). Both density dependent and independent mechanisms can affect the biomass and
543 distribution of bottom-fish (Spencer, 2008) and explain such patterns. Considering density-
544 independent mechanisms, the difference in spatial extent of the spawning area related to
545 temperature could be the result of yellowfin sole adults tracking the temperature of their preferred
546 habitat (between 1 and 7 °C, Bartolino et al. (2011); Porter (2022)). So, when bottom temperatures
547 are warm, the spawning area might extend to the western part of the inner shelf following favorable
548 temperatures that extend to the middle shelf as the cold pool contracts. Whereas cold years may
549 constrain yellowfin in shallow waters in the inner shelf (Nichol et al., 2019; Porter, 2022).

550 Our results also match patterns resulting from density-dependent mechanisms. According to the
551 theory of density-dependent habitat selection, expansion of area occupied is expected to be the
552 result of an increase in population size which reduces habitat suitability and increases competition

553 (Spencer, 2008). Our results suggest that the presence of density-dependent mechanisms seem to
554 be dependent on temperature conditions, and occur mostly during warm years. When bottom
555 temperatures are favorable (warm years), our results show an increase in density linked with an
556 increase in area occupied during the intermediate season, resulting from an expansion to suitable
557 habitats. Such mechanisms linking increase in density and spatial expansion are quite common for
558 marine species and have been observed in many systems (Scotian Shelf juvenile haddock
559 (Marshall and Frank, 1995), Atlantic cod in the southern Gulf of St. Lawrence (Swain and Wade,
560 1993), and walleye pollock (Bacheler et al., 2009)). Future studies could integrate density-
561 dependent responses with the same modelling framework used here (Thorson, 2022).

562 In addition to density independent mechanisms, a decrease in total biomass and a more constrain
563 distribution in the inner shelf during cold years can be explained by density-dependent
564 mechanisms. Indeed, between warm and cold years prey availability for yellowfin sole can change
565 in the EBS. During cold years, the cold pool extends over the middle shelf during the summer
566 season, and thus acts as a physiological barrier. Yeung et al. (2013) showed that this thermal barrier
567 displaces three flatfish species, flatfish yellowfin sole (*Limanda aspera*), Alaska plaice
568 (*Pleuronectes quadrituberculatus*) and northern rock sole (*Lepidopsetta polyxystra*) in the inner
569 shelf, intensifying competition for prey resources between those species during cold years.

570 Another potential mechanism to consider is the effect of local depletion on abundance. During
571 warm years the fishing fleet is more diffuse (less sea ice and a greater portion of the shelf open for
572 trawling), and there is less of an effect of local depletion. However, in cold years, when yellowfin
573 are more aggregated, the fishing effort and fish vulnerability increase and then local scale
574 harvesting might have a negative effect on local fish density (Bartolino et al., 2012).

575 Our results also highlight differences between males and females which are in accordance with
576 previous studies (Bartolino et al., 2011; Nichol et al., 2019). First, female distribution is more
577 expanded than male distribution and goes through the middle shelf. Then female biomass density
578 is higher than male density. Such results are in accordance with the fact that for many flatfish
579 species females grow to a larger size than males (van der Veer et al., 2001). So density-dependent
580 habitat expansion for females might be more important because of their higher energetic
581 requirements (Bartolino et al., 2011). In our study males also seem to stay longer in the spawning
582 area (especially during the warm years) than females (Nichol et al., 2019) a phenomenon largely
583 observed for flatfish (Rijnsdorp, 1989; Solmundsson et al., 2003) which results in higher overlap
584 between the survey area and fisheries CPUE for females. This can be taken into account in the
585 stock assessment by modeling sex-specific availability.

586 **A step forward to combine fishery and survey CPUE within a seasonal time step**

587 In this study, we developed a spatiotemporal model on a sub-seasonal interval to capture seasonal
588 movement based on fishery CPUE data. CPUE fishery data are of great interest to understand key
589 demographic processes and their relationship with environmental changes, and to characterize
590 essential habitats (Dambrine et al., 2021), which survey data cannot do (Suppl. Mat. S15). Fishery
591 CPUE is typically available over a large spatial domain and seasonal range, which allowed us to
592 detect phenology and time-varying availability. Fishery CPUE data were important to infer
593 spatiotemporal changes in spawning migration dynamics occurring outside the survey period.
594 These data can also be extremely useful to assess populations occurring in untrawlable habitat,
595 such as with many species of *Sebastes*. Untrawlable habitat can be a problem for estimating indices
596 of abundance from bottom trawl surveys (Jones et al., 2012, 2021; Thorson et al., 2013;

597 Zimmermann, 2003). Through cooperative research using fishing industry and community
598 knowledge of fish distribution and behavior, fishery CPUE data has the potential to improve
599 interpretation of survey-based indices of abundance (Johnson, 2011; Ressler et al., 2009).

600 However, fishery CPUE can present some limits. Fishery CPUE data might confound changes in
601 fishing behavior with trends in abundance and then are not proportional to the actual abundance.
602 We did not explicitly account for fishing behavior in this study, but we made sure that preferential
603 sampling of yellowfin fishery CPUE was low. We acknowledge that some bias might exist with
604 the actual abundance due to difference in catchability. But the goal of this study is not to provide
605 an unbiased index of abundance, rather to highlight how movement phenology, represented here
606 as seasonal hotspots in wintering, spawning, and feeding areas might change depending on
607 temperature. Accounting for scientific survey data within our approach could be complementary
608 to CPUE fishery data and provide an additional data source to estimate unbiased fish spatial
609 distribution and key demographic processes. Resource surveys for use in stock assessments are
610 typically designed to occur at approximately the same time each year (NRC, 2000), and cover a
611 large geographic area accounting for areas of few or null abundance. They also sample most of the
612 life stages of the populations providing information for characterizing the age structure and
613 population dynamics of the stocks. By using a standardized effort, they provide unbiased quantities
614 on stocks. A spatio-temporal model fitted simultaneously to fishery and survey data could be used
615 to create a joint abundance index. The joint abundance index could then be included in
616 assessments; in the example of yellowfin sole, the joint index would be an alternative to include a
617 structural linkage between summer bottom temperature and catchability.

618 Some previous studies have combined survey and fishery CPUE, accounted for seasonality, and
619 improved the estimation of the spatial distribution and abundance index of marine species
620 (Bourdaud et al., 2017; Pinto et al., 2019; Thorson, 2019b). More recently, integrated population
621 models have been developed to account for seasons explicitly (Thorson et al., 2020) and have
622 combined both fishery and survey data to account for preferential sampling in fishery CPUE data
623 (Rufener et al., 2021). Future work should focus on integrating all those data (seasonal, fishery
624 and survey CPUE, and environmental variables) within spatio-temporal models on a sub-seasonal
625 interval to capture seasonal movement. Such models will estimate the spatial distribution of each
626 species in relation to temperatures year-round, and will form the basis for a spatio-temporal
627 modeling approach to standardize the survey biomass data for each assessment. Those models
628 might also inform forecasts of future stock distribution and habitat usage under various future
629 climate and fishing pathways. In addition, the spatio-temporal modeling approach developed for
630 this project could be applied to other economically important species to inform future prediction
631 of habitat usage and distribution. In terms of management implications, this could have major
632 impacts on fishing operations and could improve our ability to estimate accurate reference points
633 in assessments.

634 **Conclusion**

635 Our study incorporates the effects of species distribution shifts into climate-ready ecosystem-based
636 fisheries management. Fishery management under global change is challenging because if
637 environmental variability ignored this could lead to overharvesting or missed harvesting
638 opportunities, changes in stock productivity, changes in life history and reductions of spawning
639 success. Our study provides a framework that could be used in climate monitoring and impact
640 analysis on fisheries. Species distribution models with spatially varying coefficients linking

641 density and environmental covariates have to be promoted to represent the response of fish to
642 environmental changes with a spatial structure (Bartolino et al., 2012, 2011; Porter and Ciannelli,
643 2018; Thorson, 2019c). Future research should be done to apply our framework to other highly
644 mobile species like flathead sole (*Hippoglossoides elassodon*), crab species in the EBS, Atlantic
645 bluefin tuna (*Thunnus thynnus*), Mediterranean albacore (*T. alalunga*), and bullet tuna (*Auxis*
646 *rochei*.) (Reglero et al., 2012; Zacher et al., 2018) to infer changes in movement phenology and
647 account for changes in availability within stock assessment to provide management approaches
648 that reduce climate-induced variability.

649

650 CREDIT AUTHORSHIP CONTRIBUTION STATEMENT

651 **Maxime Olmos:** Conceptualization (evolution of overarching research goals and aims), Formal
652 analysis, Investigation, Data curation, Methodology, Visualization, Writing – original draft.

653 **James Ianelli:** Writing, Data provision, Assessment application, Resources, Mentorship.

654 **Lorenzo Ciannelli:** Writing, Funding acquisition, Project administration, Mentorship.

655 **Ingrid Spies:** Writing, assessment application

656 **Carey R. McGilliard:** Conceptualization (Ideas), Funding acquisition, Writing, Project
657 administration, Mentorship.

658 **James T. Thorson:** Conceptualization (Ideas), Methodology, Software, Funding acquisition,
659 Writing, Project administration, Mentorship.

660

661 DECLARATION OF COMPETING INTEREST

662 The authors declare that they have no known competing financial interests or personal
663 relationships that could have appeared to influence the work reported in this paper.

664

665 FUNDING

666 Funding was provided by the National Cooperative Research Program to PIs C. McGilliard, J.
667 Thorson, and T. Essington titled "Inferring effects of loss of sea ice on movement phenology of
668 yellowfin and flathead sole in the Bering Sea and Aleutian Islands from fishery-dependent data
669 using spatio-temporal modeling". Lorenzo Ciannelli and Maxime Olmos received support from
670 the Cooperative Institute for Marine Ecosystem and Resource Studies - NOAA Cooperative
671 Agreement NA16OAR4320152 at Oregon State University.

672

673 DATA AVAILABILITY STATEMENT

674 Fisheries CPUE data are confidential data and they are available on specific request to
675 jim.ianelli@noaa.gov.

676

677 **ACKNOWLEDGEMENTS**

678 We thank the many scientists (RACE Division of the Alaska Fisheries Center) who have worked
679 long hours to provide survey data for the eastern Bering Sea. We also thank the many observers
680 and fishers that shared the fishery dependent CPUE with us. The authors also thank Arnaud
681 Grüss, Madison Hall and two anonymous reviewers whose feedbacks greatly improved the
682 manuscript.
683

684 **APPENDIX A. SUPPLEMENTARY DATA**

685 Supplementary data to this article can be found online.
686

687 **REFERENCES**

- 688 Akaike, H., 1974. A new look at the statistical model identification. *IEEE Transactions on*
689 *Automatic Control* 19, 716–723. <https://doi.org/10.1109/TAC.1974.1100705>
- 690 Akia, S., Amandé, M., Pascual, P., Gaertner, D., 2021. Seasonal and inter-annual variability in
691 abundance of the main tropical tunas in the EEZ of Côte d’Ivoire (2000-2019). *Fisheries Research*
692 243, 106053. <https://doi.org/10.1016/j.fishres.2021.106053>
- 693 Alglave, B., Rivot, E., Etienne, M.-P., Woillez, M., Thorson, J.T., Vermard, Y., 2022. Combining
694 scientific survey and commercial catch data to map fish distribution. *ICES Journal of Marine*
695 *Science fsac032*. <https://doi.org/10.1093/icesjms/fsac032>
- 696 Arnold, G.P., Metcalfe, J.D., 1996. Seasonal migrations of plaice (*Pleuronectes platessa*) through
697 the Dover Strait. *Mar. Biol.* 127, 151–160. <https://doi.org/10.1007/BF00993655>
- 698 Asch, R.G., 2015. Climate change and decadal shifts in the phenology of larval fishes in the
699 California Current ecosystem. *Proceedings of the National Academy of Sciences* 112, E4065–
700 E4074. <https://doi.org/10.1073/pnas.1421946112>
- 701 Bartolino, V., Ciannelli, L., Bacheler, N.M., Chan, K.-S., 2011. Ontogenetic and sex-specific
702 differences in density-dependent habitat selection of a marine fish population. *Ecology* 92, 189–
703 200. <https://doi.org/10.1890/09-1129.1>
- 704 Bartolino, V., Ciannelli, L., Spencer, P., Wilderbuer, T., Chan, K., 2012. Scale-dependent
705 detection of the effects of harvesting a marine fish population. *Mar. Ecol. Prog. Ser.* 444, 251–
706 261. <https://doi.org/10.3354/meps09434>

707 Bourdaud, P., Travers-Trolet, M., Vermard, Y., Cormon, X., Marchal, P., 2017. Inferring the
708 annual, seasonal, and spatial distributions of marine species from complementary research and
709 commercial vessels' catch rates. *ICES Journal of Marine Science* 74, 2415–2426.
710 <https://doi.org/10.1093/icesjms/fsx092>

711 Conn, P.B., Thorson, J.T., Johnson, D.S., 2017. Confronting preferential sampling when analysing
712 population distributions: diagnosis and model-based triage. *Methods Ecol Evol* 8, 1535–1546.
713 <https://doi.org/10.1111/2041-210X.12803>

714 Dambrine, C., Woillez, M., Huret, M., de Pontual, H., 2021. Characterising Essential Fish Habitat
715 using spatio-temporal analysis of fishery data: A case study of the European seabass spawning
716 areas. *Fisheries Oceanography* 30, 413–428. <https://doi.org/10.1111/fog.12527>

717 García Molinos, J., Halpern, B.S., Schoeman, D.S., Brown, C.J., Kiessling, W., Moore, P.J.,
718 Pandolfi, J.M., Poloczanska, E.S., Richardson, A.J., Burrows, M.T., 2016. Climate velocity and
719 the future global redistribution of marine biodiversity. *Nature Clim Change* 6, 83–88.
720 <https://doi.org/10.1038/nclimate2769>

721 Grieve, B.D., Hare, J.A., Saba, V.S., 2017. Projecting the effects of climate change on *Calanus*
722 *finmarchicus* distribution within the U.S. Northeast Continental Shelf. *Sci Rep* 7, 6264.
723 <https://doi.org/10.1038/s41598-017-06524-1>

724 Grüss, A., Gao, J., Thorson, J., Rooper, C., Thompson, G., Boldt, J., Lauth, R., 2020. Estimating
725 synchronous changes in condition and density in eastern Bering Sea fishes. *Mar. Ecol. Prog. Ser.*
726 635, 169–185. <https://doi.org/10.3354/meps13213>

727 Hartig, F., 2022. DHARMa - Residual Diagnostics for HierARchical Models.

728 Hirose, T., Minami, T., 2007. Spawning grounds and maturation status in adult flathead flounder
729 *Hippoglossoides dubius* off Niigata Prefecture, Sea of Japan. *Fisheries Sci* 73, 81–86.
730 <https://doi.org/10.1111/j.1444-2906.2007.01305.x>

731 Hoegh-Guldberg, O., Bruno, J.F., 2010. The Impact of Climate Change on the World's Marine
732 Ecosystems. *Science* 328, 1523–1528. <https://doi.org/10.1126/science.1189930>

733 Johnson, T.R., 2011. Fishermen, Scientists, and Boundary Spanners: Cooperative Research in the
734 U.S. Illex Squid Fishery. *Society & Natural Resources* 24, 242–255.
735 <https://doi.org/10.1080/08941920802545800>

736 Jones, D., Wilson, C.D., de Robertis, A., Rooper, C., 2012. Evaluation of rockfish abundance in
737 untrawlable habitat: combining acoustic and complementary sampling tools. *Fishery Bulletin*
738 1095, 14.

739 Jones, D.T., Rooper, C.N., Wilson, C.D., Spencer, P.D., Hanselman, D.H., Wilborn, R.E., 2021.
740 Estimates of availability and catchability for select rockfish species based on acoustic-optic
741 surveys in the Gulf of Alaska. *Fisheries Research* 236, 105848.
742 <https://doi.org/10.1016/j.fishres.2020.105848>

743 Kai, M., Thorson, J.T., Piner, K.R., Maunder, M.N., 2017. Predicting the spatio-temporal
744 distributions of pelagic sharks in the western and central North Pacific. *Fisheries Oceanography*
745 26, 569–582. <https://doi.org/10.1111/fog.12217>

746 Kanamori, Y., Takasuka, A., Nishijima, S., Okamura, H., 2019. Climate change shifts the
747 spawning ground northward and extends the spawning period of chub mackerel in the western
748 North Pacific. *Mar. Ecol. Prog. Ser.* 624, 155–166. <https://doi.org/10.3354/meps13037>

749 Kneebone, J., Bowlby, H., Mello, J.J., McCandless, C.T., Natanson, L.J., Gervelis, B., Skomal,
750 G.B., Kohler, N., Bernal, D., 2020. Seasonal distribution and habitat use of the common thresher
751 shark (*Alopias vulpinus*) in the western North Atlantic Ocean inferred from fishery-dependent
752 data. *FB* 118, 399–411. <https://doi.org/10.7755/FB.118.4.8>

753 Kovach, R.P., Ellison, S.C., Pyare, S., Tallmon, D.A., 2015. Temporal patterns in adult salmon
754 migration timing across southeast Alaska. *Global Change Biology* 21, 1821–1833.
755 <https://doi.org/10.1111/gcb.12829>

756 Kristensen, K., Nielsen, A., Berg, C.W., Skaug, H., Bell, B.M., 2016. TMB: Automatic
757 Differentiation and Laplace Approximation. *Journal of Statistical Software* 70.
758 <https://doi.org/10.18637/jss.v070.i05>

759 Lindgren, 2012. Continuous domain spatial models in R-INLA. *The ISBA Bulletin* 19, 14–20.

760 Loher, T., 2011. Analysis of match–mismatch between commercial fishing periods and spawning
761 ecology of Pacific halibut (*Hippoglossus stenolepis*), based on winter surveys and behavioural data
762 from electronic archival tags. *ICES Journal of Marine Science* 68, 2240–2251.
763 <https://doi.org/10.1093/icesjms/fsr152>

764 Maunder, M.N., Sibert, J.R., Fonteneau, A., Hampton, J., Kleiber, P., Harley, S.J., 2006.
765 Interpreting catch per unit effort data to assess the status of individual stocks and communities.
766 *ICES Journal of Marine Science* 63, 1373–1385. <https://doi.org/10.1016/j.icesjms.2006.05.008>

767 McQueen, K., Marshall, C.T., 2017. Shifts in spawning phenology of cod linked to rising sea
768 temperatures. *ICES Journal of Marine Science* 74, 1561–1573.
769 <https://doi.org/10.1093/icesjms/fsx025>

770 Monnahan, C.C., Branch, T.A., Thorson, J.T., Stewart, I.J., Szuwalski, C.S., 2019. Overcoming
771 long Bayesian run times in integrated fisheries stock assessments. *ICES Journal of Marine Science*
772 76, 1477–1488. <https://doi.org/10.1093/icesjms/fsz059>

773 Monnahan, C.C., Kristensen, K., 2018. No-U-turn sampling for fast Bayesian inference in ADMB
774 and TMB: Introducing the adnuts and tmbstan R packages. *PLOS ONE* 13, e0197954.
775 <https://doi.org/10.1371/journal.pone.0197954>

776 Mundy, P.R., Evenson, D.F., 2011. Environmental controls of phenology of high-latitude Chinook
777 salmon populations of the Yukon River, North America, with application to fishery management.
778 *ICES Journal of Marine Science* 68, 1155–1164. <https://doi.org/10.1093/icesjms/fsr080>

779 Murray, L.G., Hinz, H., Hold, N., Kaiser, M.J., 2013. The effectiveness of using CPUE data
780 derived from Vessel Monitoring Systems and fisheries logbooks to estimate scallop biomass. *ICES*
781 *Journal of Marine Science* 70, 1330–1340. <https://doi.org/10.1093/icesjms/fst099>

782 Myers, R.A., Worm, B., 2003. Rapid worldwide depletion of predatory fish communities. *Nature*
783 423, 280–283. <https://doi.org/10.1038/nature01610>

784 Neidetcher, S.K., Hurst, T.P., Ciannelli, L., Logerwell, E.A., 2014. Spawning phenology and
785 geography of Aleutian Islands and eastern Bering Sea Pacific cod (*Gadus macrocephalus*). *Deep*
786 *Sea Research Part II: Topical Studies in Oceanography, Understanding Ecosystem Processes in*
787 *the Eastern Bering Sea III* 109, 204–214. <https://doi.org/10.1016/j.dsr2.2013.12.006>

788 Nichol, D., 1998. Annual and between-sex variability of yellowfin sole, *Pleuronectes aspe*, spring-
789 summer distributions in the eastern Bering Sea. *Fish. Bull., U.S.* 96, 547–561.

790 Nichol, D., 1995. Spawning and maturation of female yellowfin sole in the eastern Bering Sea.
791 *Proceedings of the International Flatfish Symposium: October 1994, Anchorage* 35–50.

792 Nichol, D.G., Kotwicki, S., Wilderbuer, T.K., Lauth, R.R., Ianelli, J.N., 2019. Availability of
793 yellowfin sole *Limanda aspera* to the eastern Bering Sea trawl survey and its effect on estimates
794 of survey biomass. *Fisheries Research* 211, 319–330.
795 <https://doi.org/10.1016/j.fishres.2018.11.017>

796 NRC, N.R.C., 2000. *Improving the Collection, Management, and Use of Marine Fisheries Data.*
797 National Academies Press, Washington, D.C. <https://doi.org/10.17226/9969>

798 Otero, J., L'Abée-Lund, J.H., Castro-Santos, T., Leonardsson, K., Storvik, G.O., Jonsson, B.,
799 Dempson, B., Russell, I.C., Jensen, A.J., Baglinière, J.-L., Dionne, M., Armstrong, J.D.,
800 Romakkaniemi, A., Letcher, B.H., Kocik, J.F., Erkinaro, J., Poole, R., Rogan, G., Lundqvist, H.,
801 MacLean, J.C., Jokikokko, E., Arnekleiv, J.V., Kennedy, R.J., Niemelä, E., Caballero, P., Music,
802 P.A., Antonsson, T., Gudjonsson, S., Veselov, A.E., Lamberg, A., Groom, S., Taylor, B.H.,
803 Taberner, M., Dillane, M., Arnason, F., Horton, G., Hvidsten, N.A., Jonsson, I.R., Jonsson, N.,
804 McKelvey, S., Naesje, T.F., Skaala, Ø., Smith, G.W., Saegrov, H., Stenseth, N.C., Vøllestad, L.A.,
805 2014. Basin-scale phenology and effects of climate variability on global timing of initial seaward
806 migration of Atlantic salmon (*Salmo salar*). *Global Change Biology* 20, 61–75.
807 <https://doi.org/10.1111/gcb.12363>

808 Parmesan, C., Yohe, G., 2003. A globally coherent fingerprint of climate change impacts across
809 natural systems. *Nature* 421, 37–42. <https://doi.org/10.1038/nature01286>

810 Pauly, D., Christensen, V., Dalsgaard, J., Froese, R., Torres, F., 1998. Fishing Down Marine Food
811 Webs. *Science* 279, 860–863. <https://doi.org/10.1126/science.279.5352.860>

812 Peer, A.C., Miller, T.J., 2014. Climate Change, Migration Phenology, and Fisheries Management
813 Interact with Unanticipated Consequences. *North American Journal of Fisheries Management* 34,
814 94–110. <https://doi.org/10.1080/02755947.2013.847877>

815 Pennino, M.G., Conesa, D., López-Quílez, A., Muñoz, F., Fernández, A., Bellido, J.M., 2016.
816 Fishery-dependent and -independent data lead to consistent estimations of essential habitats. ICES
817 Journal of Marine Science 73, 2302–2310. <https://doi.org/10.1093/icesjms/fsw062>

818 Pinto, C., Travers-Trolet, M., Macdonald, J.I., Rivot, E., Vermard, Y., 2019. Combining multiple
819 data sets to unravel the spatiotemporal dynamics of a data-limited fish stock. Can. J. Fish. Aquat.
820 Sci. 76, 1338–1349. <https://doi.org/10.1139/cjfas-2018-0149>

821 Poloczanska, E.S., Brown, C.J., Sydeman, W.J., Kiessling, W., Schoeman, D.S., Moore, P.J.,
822 Brander, K., Bruno, J.F., Buckley, L.B., Burrows, M.T., Duarte, C.M., Halpern, B.S., Holding, J.,
823 Kappel, C.V., O'Connor, M.I., Pandolfi, J.M., Parmesan, C., Schwing, F., Thompson, S.A.,
824 Richardson, A.J., 2013. Global imprint of climate change on marine life. Nature Climate Change
825 3, 919–925. <https://doi.org/10.1038/nclimate1958>

826 Porter, S.M., Ciannelli, L., 2018. Effect of temperature on Flathead Sole (*Hippoglossoides*
827 *elassodon*) spawning in the southeastern Bering Sea during warm and cold years. Journal of Sea
828 Research 141, 26–36. <https://doi.org/10.1016/j.seares.2018.08.003>

829 Reglero, P., Ciannelli, L., Alvarez-Berastegui, D., Balbín, R., López-Jurado, J., Alemany, F., 2012.
830 Geographically and environmentally driven spawning distributions of tuna species in the western
831 Mediterranean Sea. Mar. Ecol. Prog. Ser. 463, 273–284. <https://doi.org/10.3354/meps09800>

832 Ressler, P.H., Fleischer, G.W., Wespestad, V.G., Harms, J., 2009. Developing a commercial-
833 vessel-based stock assessment survey methodology for monitoring the U.S. west coast widow
834 rockfish (*Sebastes entomelas*) stock. Fisheries Research 99, 63–73.
835 <https://doi.org/10.1016/j.fishres.2009.04.008>

836 Rijnsdorp, A.D., 1989. Maturation of male and female North Sea plaice (*Pleuronectes platessa* L.).
837 ICES Journal of Marine Science 46, 35–51. <https://doi.org/10.1093/icesjms/46.1.35>

838 Rogers, L.A., Dougherty, A.B., 2019. Effects of climate and demography on reproductive
839 phenology of a harvested marine fish population. Glob Change Biol 25, 708–720.
840 <https://doi.org/10.1111/gcb.14483>

841 Rufener, M.-C., Kristensen, K., Nielsen, J.R., Bastardie, F., 2021. Bridging the gap between
842 commercial fisheries and survey data to model the spatiotemporal dynamics of marine species.
843 *Ecological Applications* 31, e02453. <https://doi.org/10.1002/eap.2453>

844 Sims, D.W., Wearmouth, V.J., Genner, M.J., Southward, A.J., Hawkins, S.J., 2004. Low-
845 temperature-driven early spawning migration of a temperate marine fish. *Journal of Animal*
846 *Ecology* 73, 333–341. <https://doi.org/10.1111/j.0021-8790.2004.00810.x>

847 Solmundsson, J., Karlsson, H., Palsson, J., 2003. Sexual differences in spawning behaviour and
848 catchability of plaice (*Pleuronectes platessa*) west of Iceland. *Fisheries Research* 61, 57–71.
849 [https://doi.org/10.1016/S0165-7836\(02\)00212-6](https://doi.org/10.1016/S0165-7836(02)00212-6)

850 Spies, I., Wilderbuer, T., Nichol, D., Ianelli, J., 2019. Assessment of the Yellowfin Sole Stock in
851 the Bering Sea and Aleutian Islands North Pacific Fishery Management Council, 88.

852 Staudinger, M.D., Mills, K.E., Stamieszkin, K., Record, N.R., Hudak, C.A., Allyn, A., Diamond,
853 A., Friedland, K.D., Golet, W., Henderson, M.E., Hernandez, C.M., Huntington, T.G., Ji, R.,
854 Johnson, C.L., Johnson, D.S., Jordaan, A., Kocik, J., Li, Y., Liebman, M., Nichols, O.C.,
855 Pendleton, D., Richards, R.A., Robben, T., Thomas, A.C., Walsh, H.J., Yakola, K., 2019. It's about
856 time: A synthesis of changing phenology in the Gulf of Maine ecosystem. *Fisheries Oceanography*
857 28, 532–566. <https://doi.org/10.1111/fog.12429>

858 Swain, D.P., Wade, E.J., 2003. Spatial distribution of catch and effort in a fishery for snow crab (
859 *Chionoecetes opilio*): tests of predictions of the ideal free distribution. *Can. J. Fish. Aquat. Sci.*
860 60, 897–909. <https://doi.org/10.1139/f03-076>

861 Sydeman, W.J., Poloczanska, E., Reed, T.E., Thompson, S.A., 2015. Climate change and marine
862 vertebrates. *Science* 350, 772–777. <https://doi.org/10.1126/science.aac9874>

863 Thorson, J.T., 2022. Development and simulation testing for a new approach to density
864 dependence in species distribution models. *ICES Journal of Marine Science* 79, 117–128.
865 <https://doi.org/10.1093/icesjms/fsab247>

866 Thorson, J.T., 2019a. Measuring the impact of oceanographic indices on species distribution shifts:
867 The spatially varying effect of cold-pool extent in the eastern Bering Sea. *Limnology and*
868 *Oceanography* 64, 2632–2645. <https://doi.org/10.1002/lno.11238>

869 Thorson, J.T., 2019b. Guidance for decisions using the Vector Autoregressive Spatio-Temporal
870 (VAST) package in stock, ecosystem, habitat and climate assessments. *Fisheries Research* 210,
871 143–161. <https://doi.org/10.1016/j.fishres.2018.10.013>

872 Thorson, J.T., 2019c. Measuring the impact of oceanographic indices on species distribution shifts:
873 The spatially varying effect of cold-pool extent in the eastern Bering Sea. *Limnology and*
874 *Oceanography* 64, 2632–2645. <https://doi.org/10.1002/lno.11238>

875 Thorson, J.T., Adams, C.F., Brooks, E.N., Eisner, L.B., Kimmel, D.G., Legault, C.M., Rogers,
876 L.A., Yasumiishi, E.M., 2020. Seasonal and interannual variation in spatio-temporal models for
877 index standardization and phenology studies. *ICES Journal of Marine Science* 77, 1879–1892.
878 <https://doi.org/10.1093/icesjms/fsaa074>

879 Thorson, J.T., Ianelli, J.N., Larsen, E.A., Ries, L., Scheuerell, M.D., Szuwalski, C., Zipkin, E.F.,
880 2016. Joint dynamic species distribution models: a tool for community ordination and spatio-
881 temporal monitoring. *Global Ecology and Biogeography* 25, 1144–1158.
882 <https://doi.org/10.1111/geb.12464>

883 Thorson, J.T., M. Elizabeth, C., Stewart, I.J., Punt, A.E., 2013. The implications of spatially
884 varying catchability on bottom trawl surveys of fish abundance: a proposed solution involving
885 underwater vehicles. *Can. J. Fish. Aquat. Sci.* 70, 294–306.

886 van der Veer, H.W., Kooijman, S.A.L.M., van der Meer, J., 2001. Intra- and interspecies
887 comparison of energy flow in North Atlantic flatfish species by means of dynamic energy budgets.
888 *Journal of Sea Research* 45, 303–320. [https://doi.org/10.1016/S1385-1101\(01\)00061-2](https://doi.org/10.1016/S1385-1101(01)00061-2)

889 Wakabayashi, K., 1989. Studies on the fishery biology of yellowfin sole [*Limanda aspera*] in the
890 eastern Bering Sea. *Bulletin - Far Seas Fisheries Research Laboratory (Japan)*.

891 Walters, C., 2003. Folly and fantasy in the analysis of spatial catch rate data. *Can. J. Fish. Aquat.*
892 *Sci.* 60, 1433–1436. <https://doi.org/10.1139/f03-152>

893 Walters, C.J., Hilborn, R., 2005. Exploratory assessment of historical recruitment patterns using
894 relative abundance and catch data. *Can. J. Fish. Aquat. Sci.* 62, 1985–1990.
895 <https://doi.org/10.1139/f05-105>

896 Wilderbuer, T., Walters, G., Bakkala, R., 1992. Yellowfin sole, *Pleuronectes asper*, of the eastern
897 Bering Sea : biological characteristics, history of exploitation, and management *Marine Fisheries*
898 *Review* 54(4):1–18.

899 Yeung, C., Yang, M.-S., Jewett, S.C., Naidu, A.S., 2013. Polychaete assemblage as surrogate for
900 prey availability in assessing southeastern Bering Sea flatfish habitat. *Journal of Sea Research* 76,
901 211–221. <https://doi.org/10.1016/j.seares.2012.09.008>

902 Zacher, L.S., Kruse, G.H., Hardy, S.M., 2018. Autumn distribution of Bristol Bay red king crab
903 using fishery logbooks. *PLOS ONE* 13, e0201190. <https://doi.org/10.1371/journal.pone.0201190>

904 Zimmermann, M., 2003. Calculation of untrawlable areas within the boundaries of a bottom trawl
905 survey 60, 13.

906

907

908
909

Table 1: Summary of the hypotheses tested, the associated model configurations and AIC values attributed to each model. ΔAIC is the difference in AIC score between the best model and the model being compared

Models	Spatiotemporal variations in CPUE are explained by	Ecological hypothesis	Equations	ΔAIC
M0	Year effect, Spatial main effect, and year spatial effect	Does not account for seasonality and interannual temperature changes	$\log [b(s_i, t_i)] = \beta(t_i) + \omega(s_i) + \varepsilon(s_i, t_i)$	658
M1	M0 + spatial effect of seasons u , on CPUE	Account for seasonality, (i.e changes in movement phenology) but not interannual temperature changes	$\log [b(s_i, t_i)] = \beta(t_i) + \sum ((\lambda(k_u) + \varphi(s_i, k_u))q(i, k_u)) + \omega(s_i) + \varepsilon(s_i, t_i)$ With $u = c(Early, Intermediate, Late)$	654
M2	M0 + spatial effect of interannual temperature changes v	Account for impact of interannual temperature changes, but not for seasonality	$\log [b(s_i, t_i)] = \beta(t_i) + \sum ((\lambda(k_{v(t)}) + \varphi(s_i, k_{v(t)}))q(i, k_{v(t)})) + \omega(s_i) + \varepsilon(s_i, t_i)$ With $v = c(Cold, Warm)$	170
M3	M0 + spatial effect of the interaction of seasons u and interannual temperature changes v	Account for changes in movement phenology in response to interannual temperature changes	$\log [b(s_i, t_i)] = \beta(t_i) + \sum ((\lambda(k_{u,v(t)}) + \varphi(s_i, k_{u,v(t)}))q(i, k_{u,v(t)})) + \omega(s_i) + \varepsilon(s_i, t_i)$ With $v = c(Cold, Warm)$ and $u = c(Early, Intermediate, Late)$	0

910

911

912

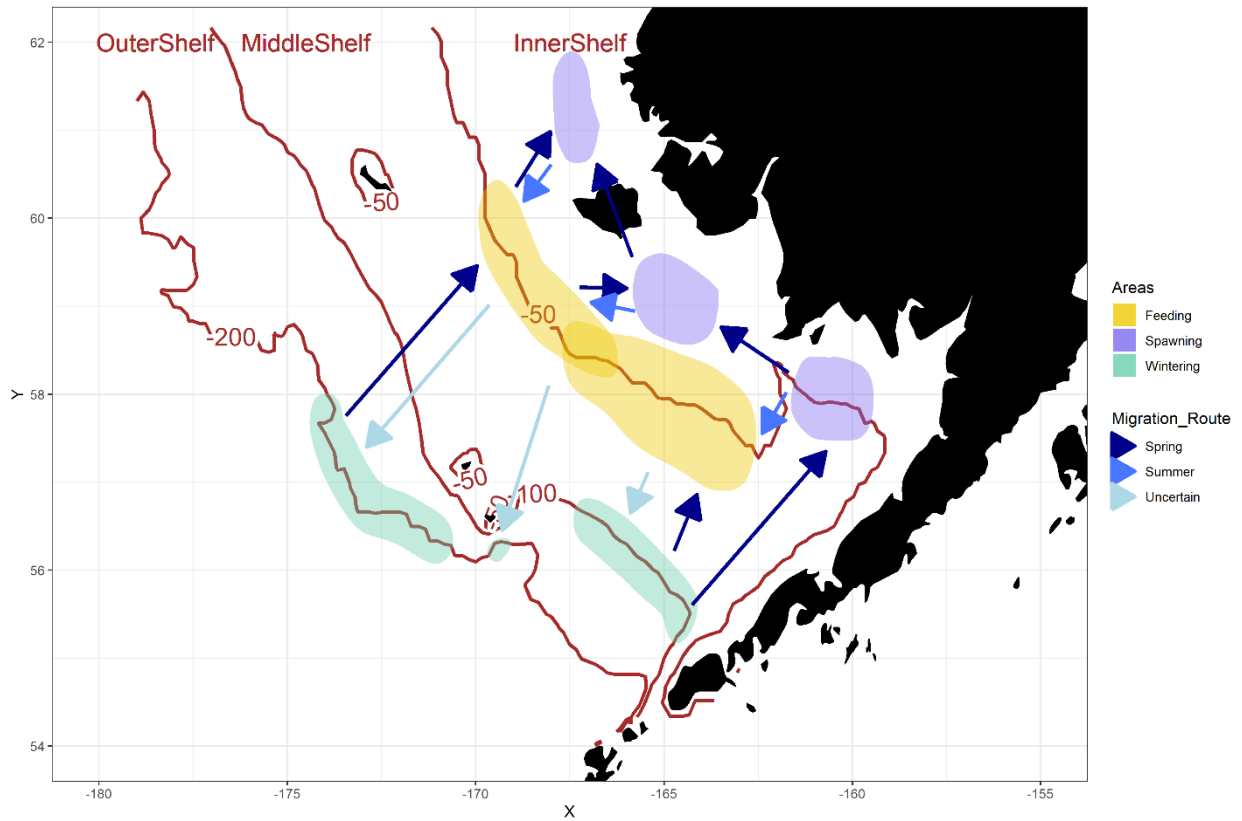


Figure 1: Distribution of wintering, spawning, and feeding areas for yellowfin sole in the Bering Sea, and observed regional grouping. Migration routes from wintering to feeding take place in spring, and the dates that Yellowfin Sole return to their wintering areas are unknown. Outer, middle, and inner shelf are defined for bathymetry between 200-100 meters, 100-50 meters and <50 meters respectively. (Adapted from Wakabayashi (1989) and Spies et al. (2019))

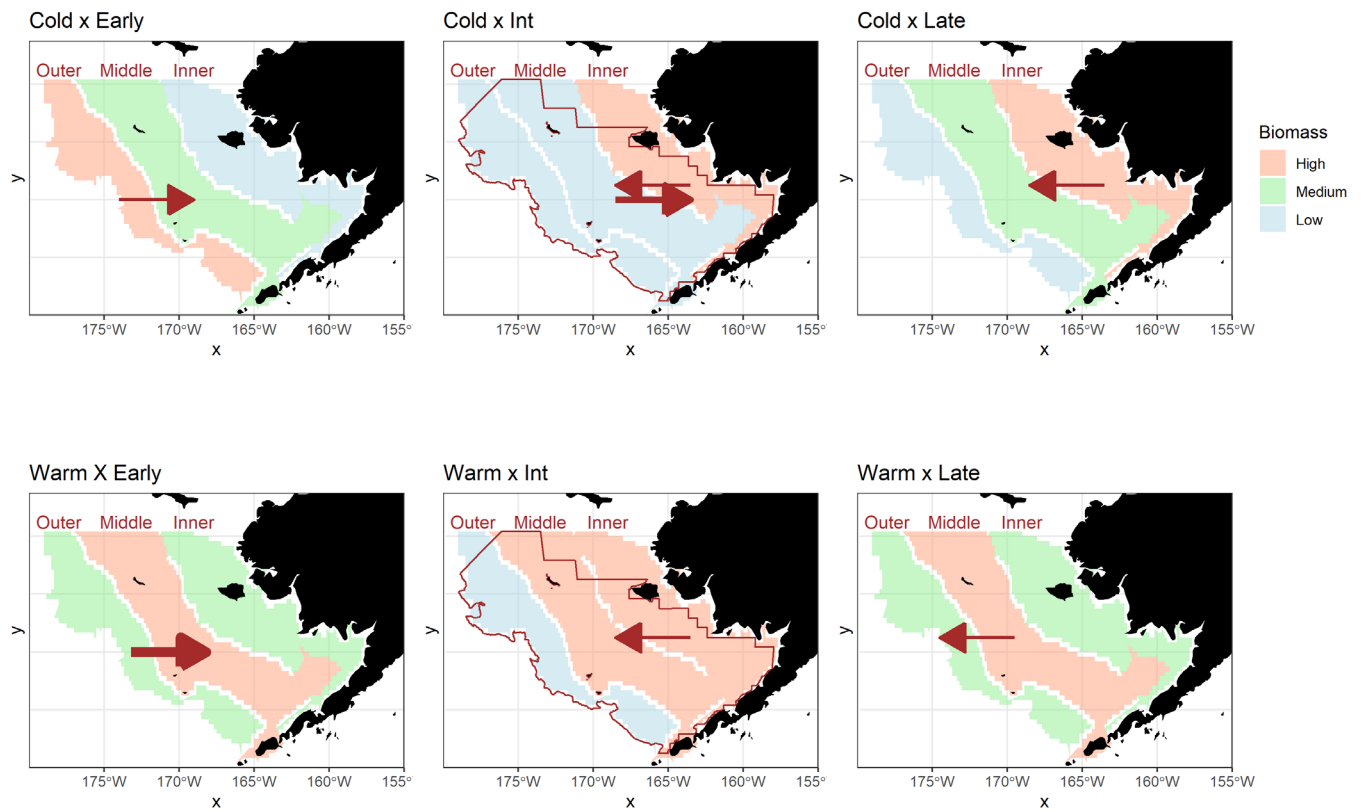


Figure 2: Conceptual expectation about how temperature changes (warm or cold years) and seasons (Early, Intermediate, Late) may affect the spatial distribution of biomass. Survey area (brown lines) is represented when survey occurs during the intermediate season. Brown arrows represent the hypothesized ontogenetic migrations (the thickness represents the intensity of the migration in term of biomass).

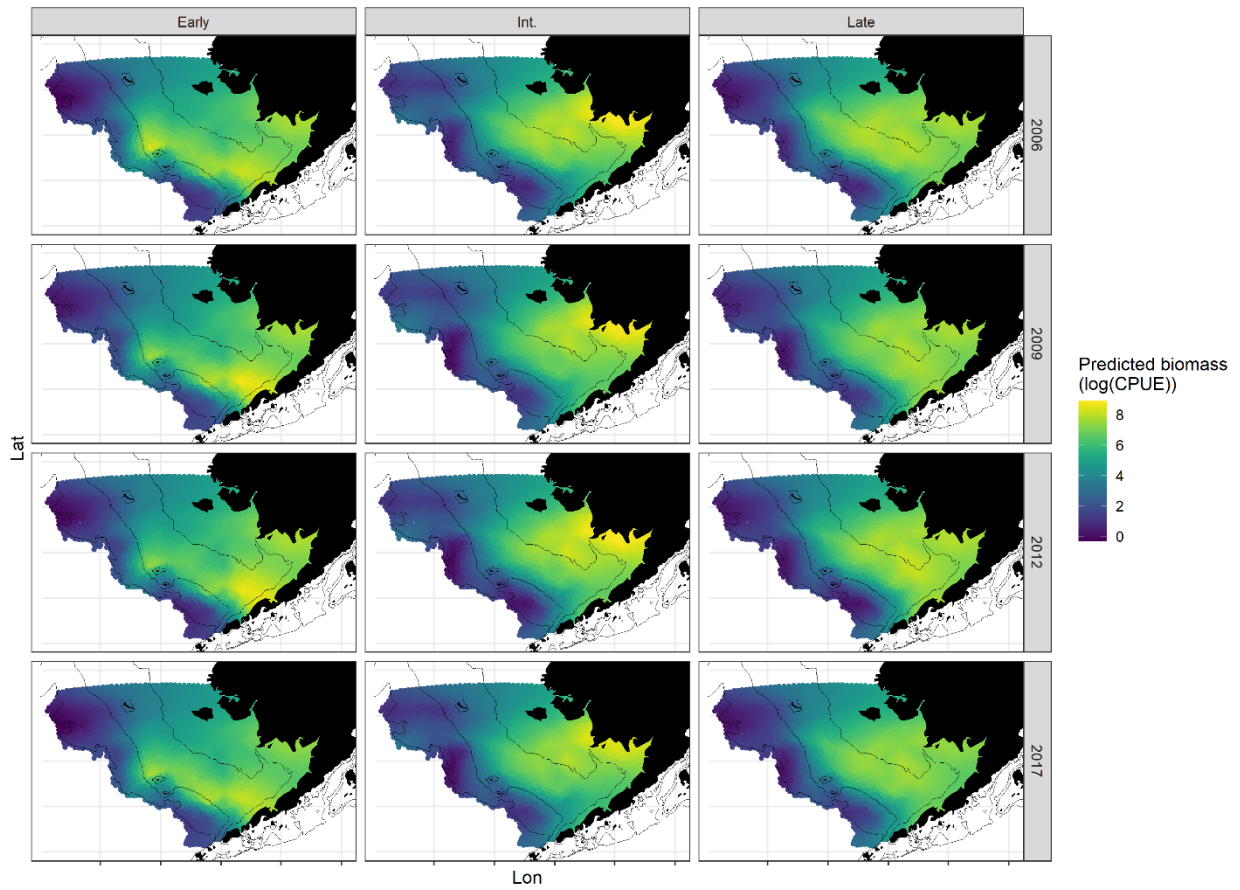


Figure 3: Seasonal spatiotemporal distribution of CPUE. Seasons are defined as Early, Intermediate (Int.) and Late) (Years 2006, 2009, 2012, 2017 (cold years) are chosen as example because seasonality changes are more pronounced for cold years). Full panels are in Suppl. Mat. Fig. S12.

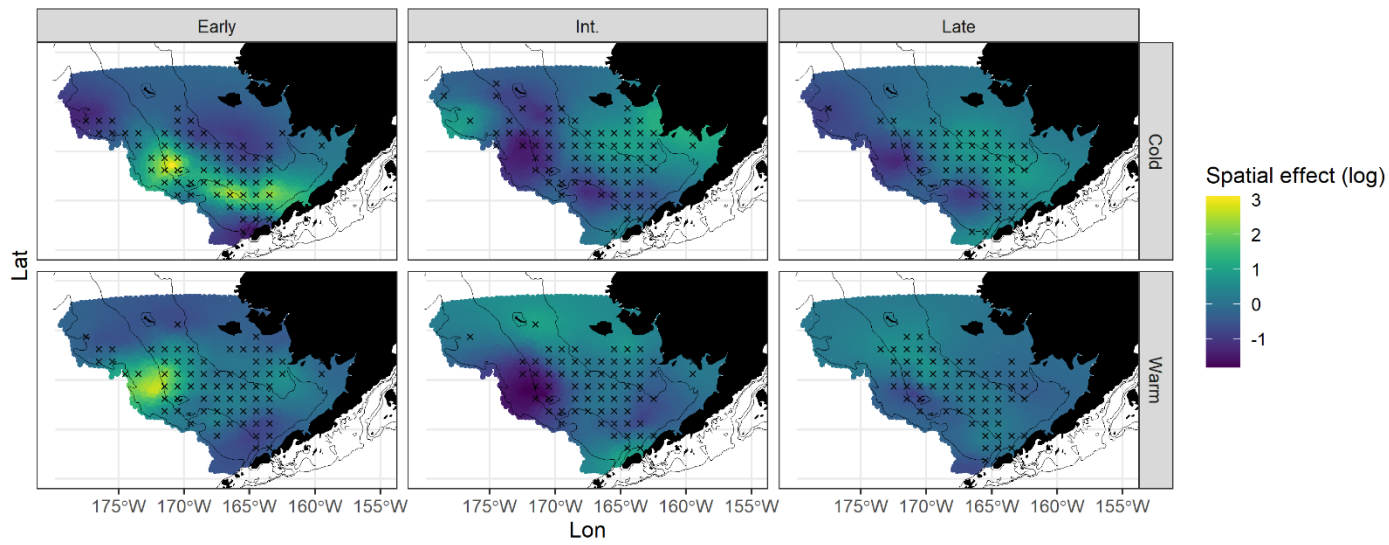


Figure 4: Spatial variation covariate effects φ on fisheries CPUE. Covariates represent the combined effect of *season* and *temperature* (ColdEarly, ColdIntermediate, ColdLate, WarmEarly, WarmIntermediate, WarmLate). Black crosses represent the spatial distribution of the data for each combination of *season* and *temperature* when aggregating across years. The model uses a log-link such that a location with value 0.1 is expected to have a $\exp(0.1) \approx 10\%$ higher expected CPUE than a location with value 0.

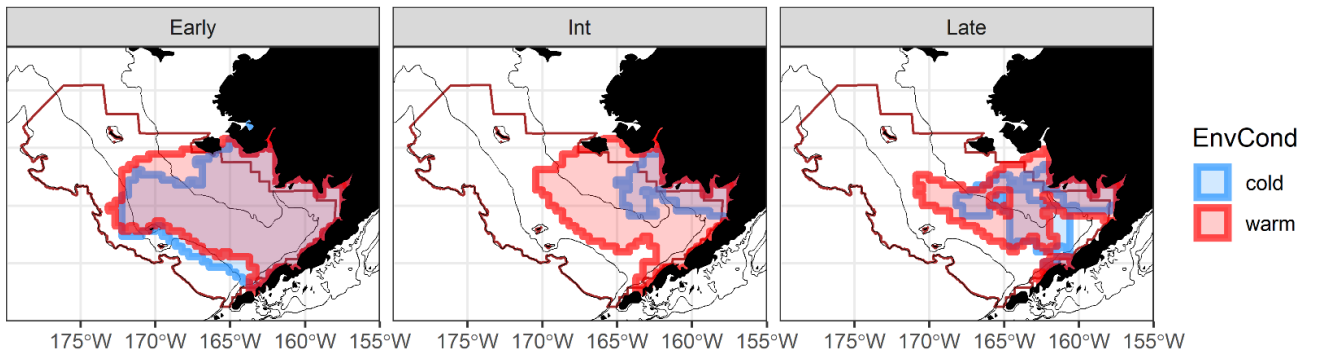


Figure 5: Seasonal spatial biomass distribution of yellowfin sole averaged for warm years (red) and cold years (blue). Red and blue polygons represent the cumulative biomass including 95% of the total biomass ($b(s, u, v^*)$ Eq. 5) across the entire spatial area for warm and cold years respectively and for each season. Brown polygon represents the survey area.

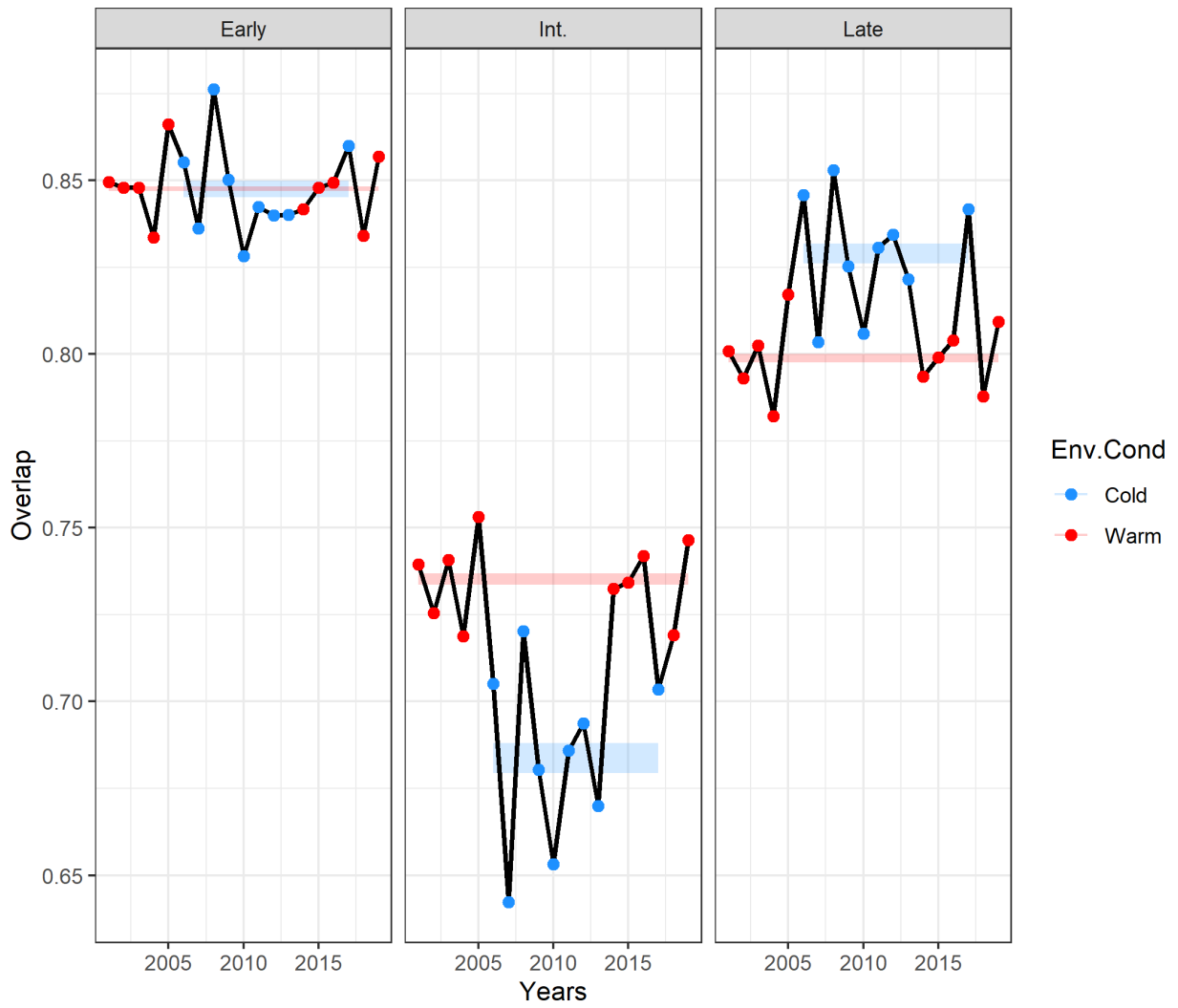


Figure 6: Time series of the overlap between spatial distribution of fishery CPUE biomass and survey spatial footprint during the different seasons (columns) Thick lines represent the averaged overlap across years (thickness of the line represents the standard deviation).

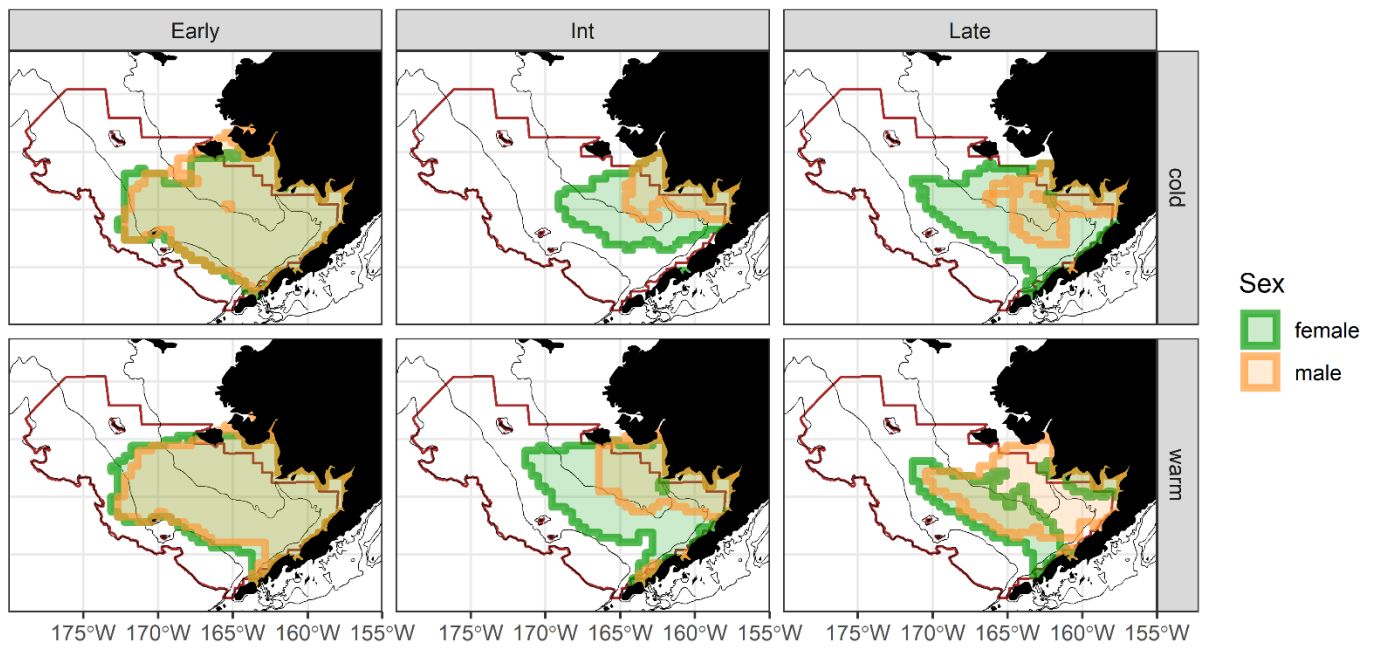


Figure 7: Mean seasonal spatial biomass distribution of yellowfin sole for cold years (1st row) and warm years (second row) for females and males. Green and orange polygons represent the cumulative biomass including the 95% of the total biomass across the entire spatial area for females and males respectively and for each season. Brown polygon represents the survey area.

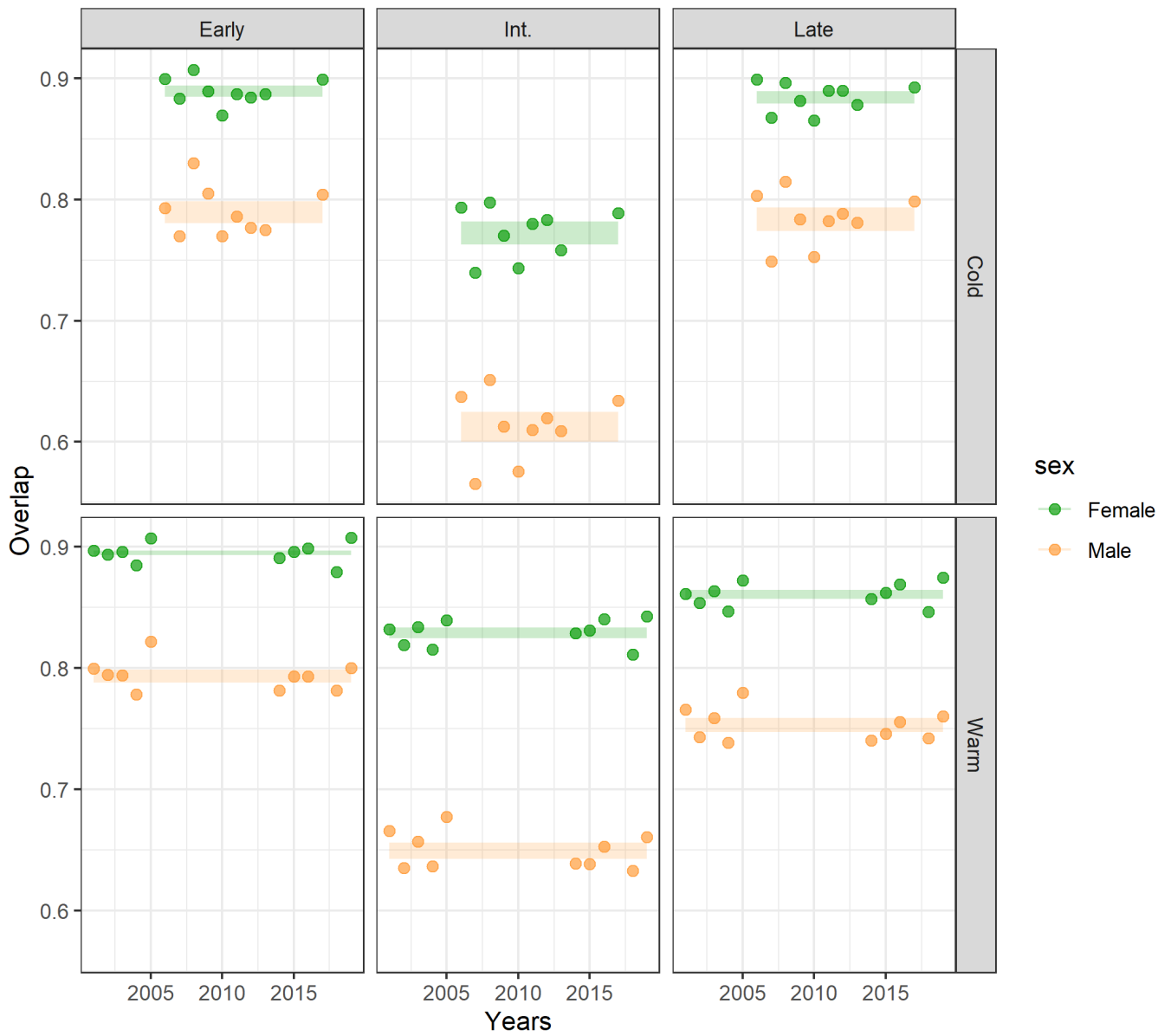


Figure 8: Time series between spatial distribution of fishery CPUE biomass and survey spatial footprint for females (orange) and males (green) during the different seasons (columns) and in cold and warm years (rows). Thick lines represent the average overlap across years (thickness of the line represent the standard deviation).

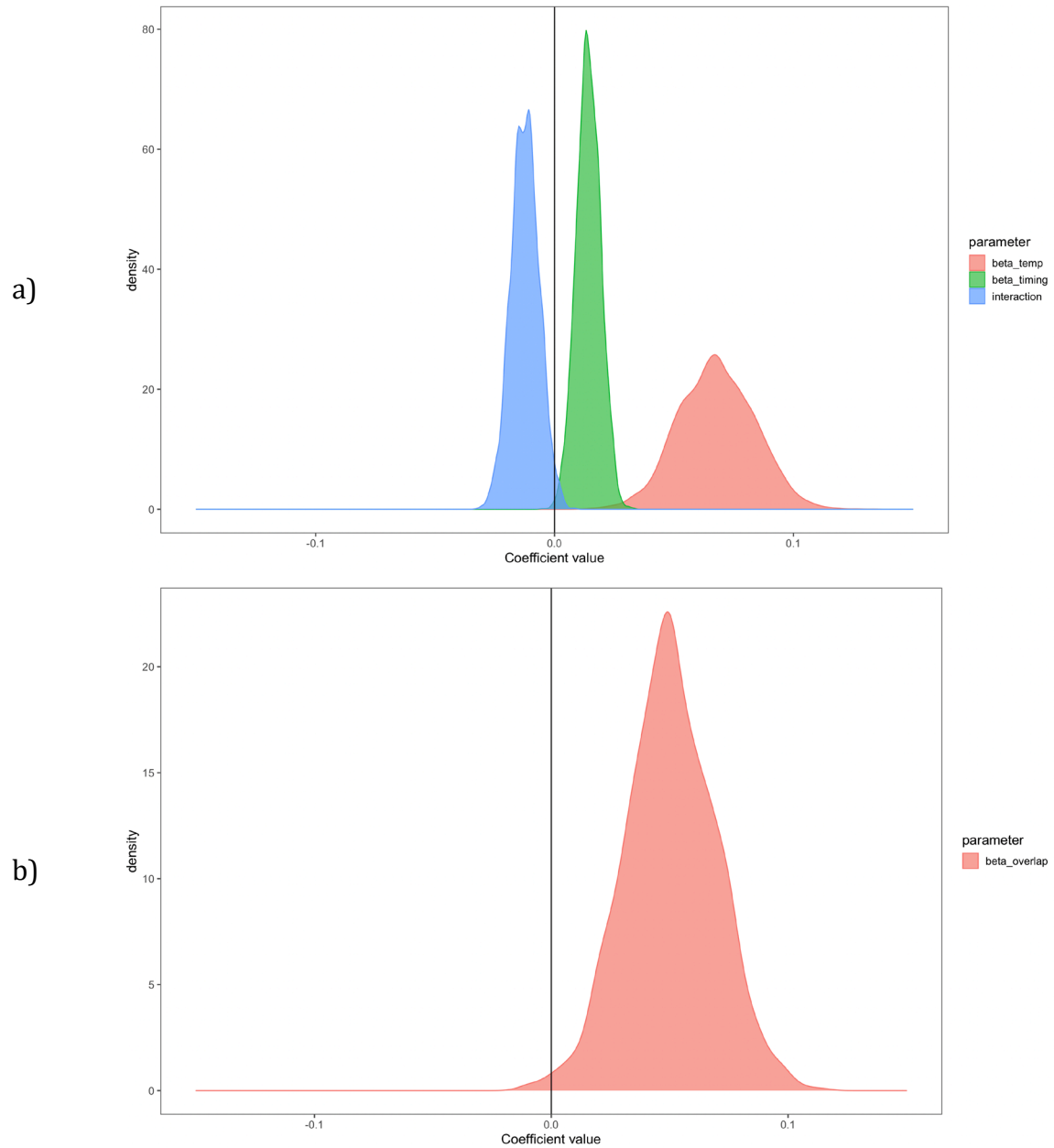


Figure 9: Posterior densities of coefficients as estimated from the stock assessment model (Spies et al. 2021) for model SAM.1 (panel a), and for the new overlap index, SAM.2, “beta_overlap” (panel b). These coefficients affect survey catchability (availability) applied to zero-centered anomalies.

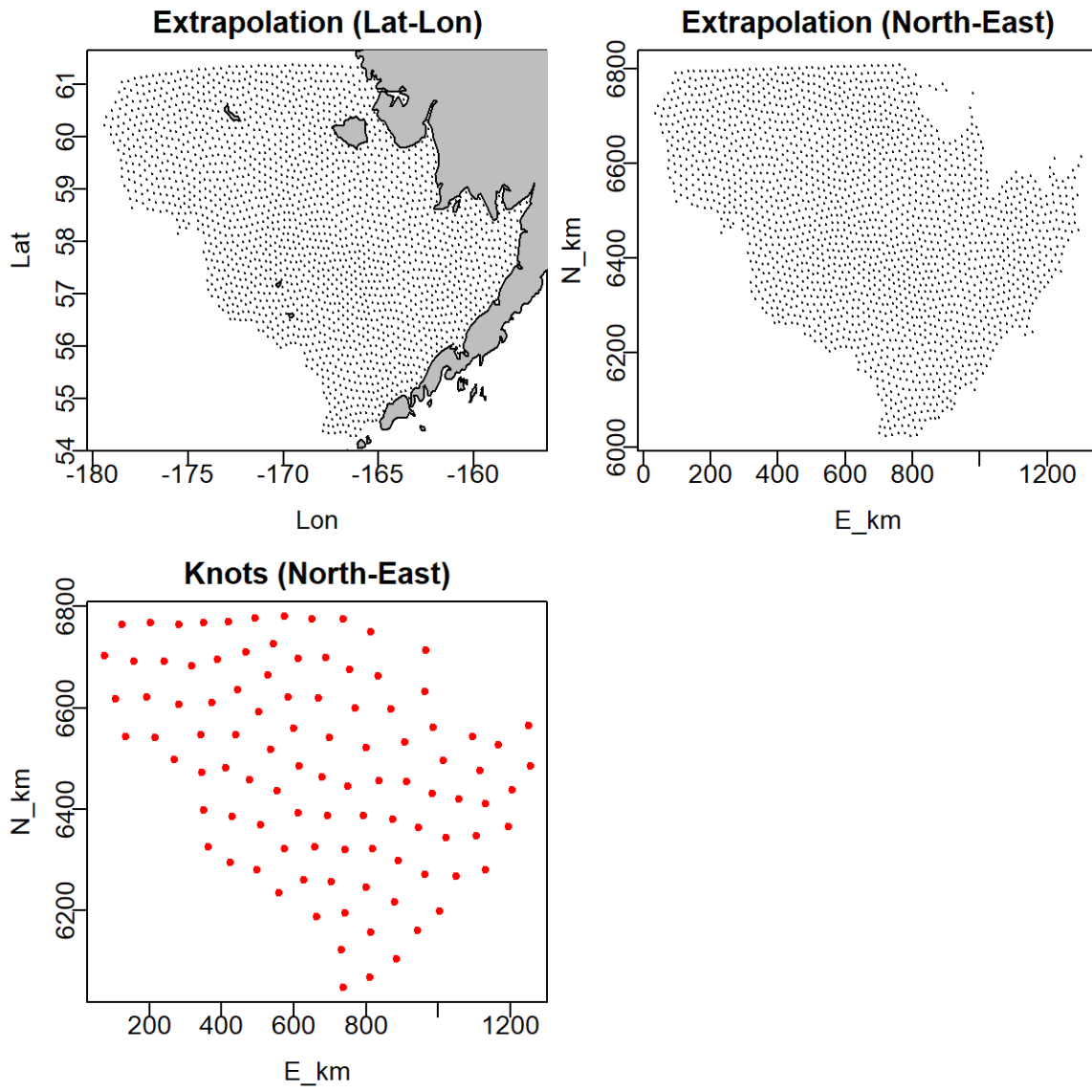


Figure S1: Spatial resolution of the study. Extrapolation grid and spatial distribution of the knots.

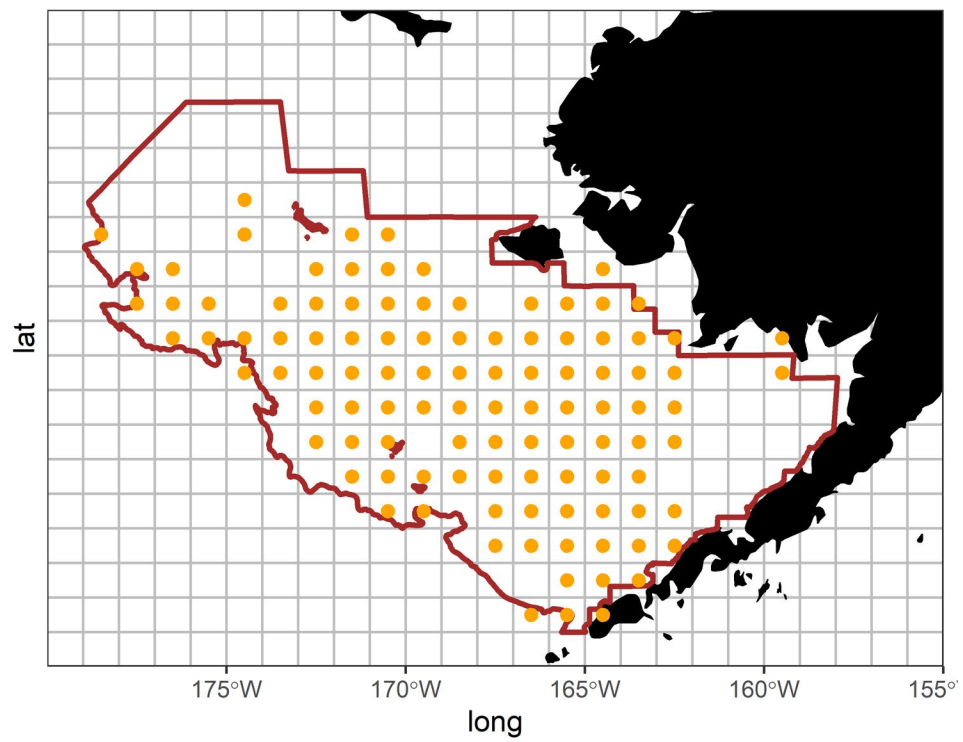
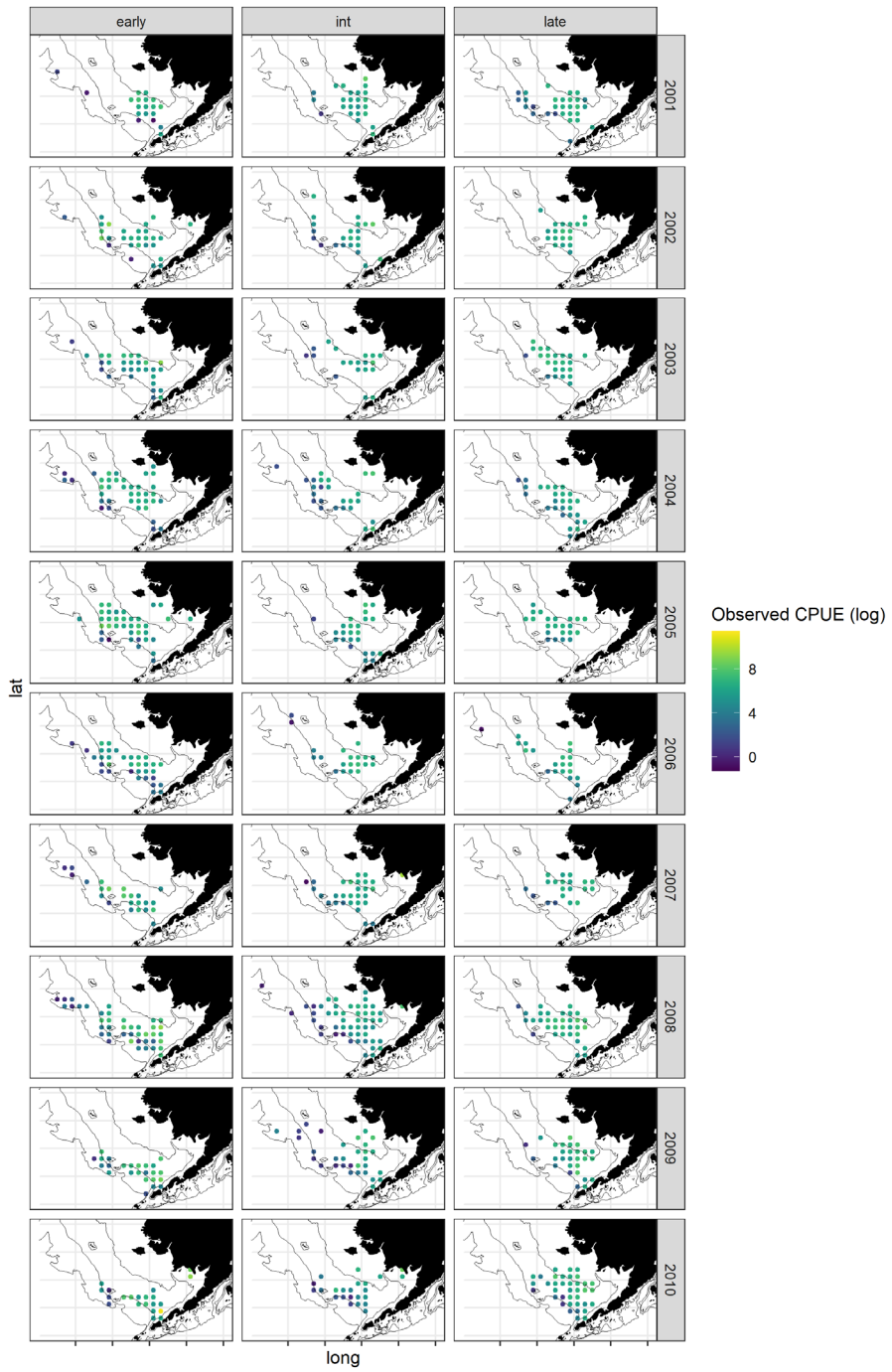


Figure S2: Spatial resolution of data. Grid represents the ADFG cells. Brown polygon is the survey area. And orange dots are the location of fisheries CPUE (2001-2019)



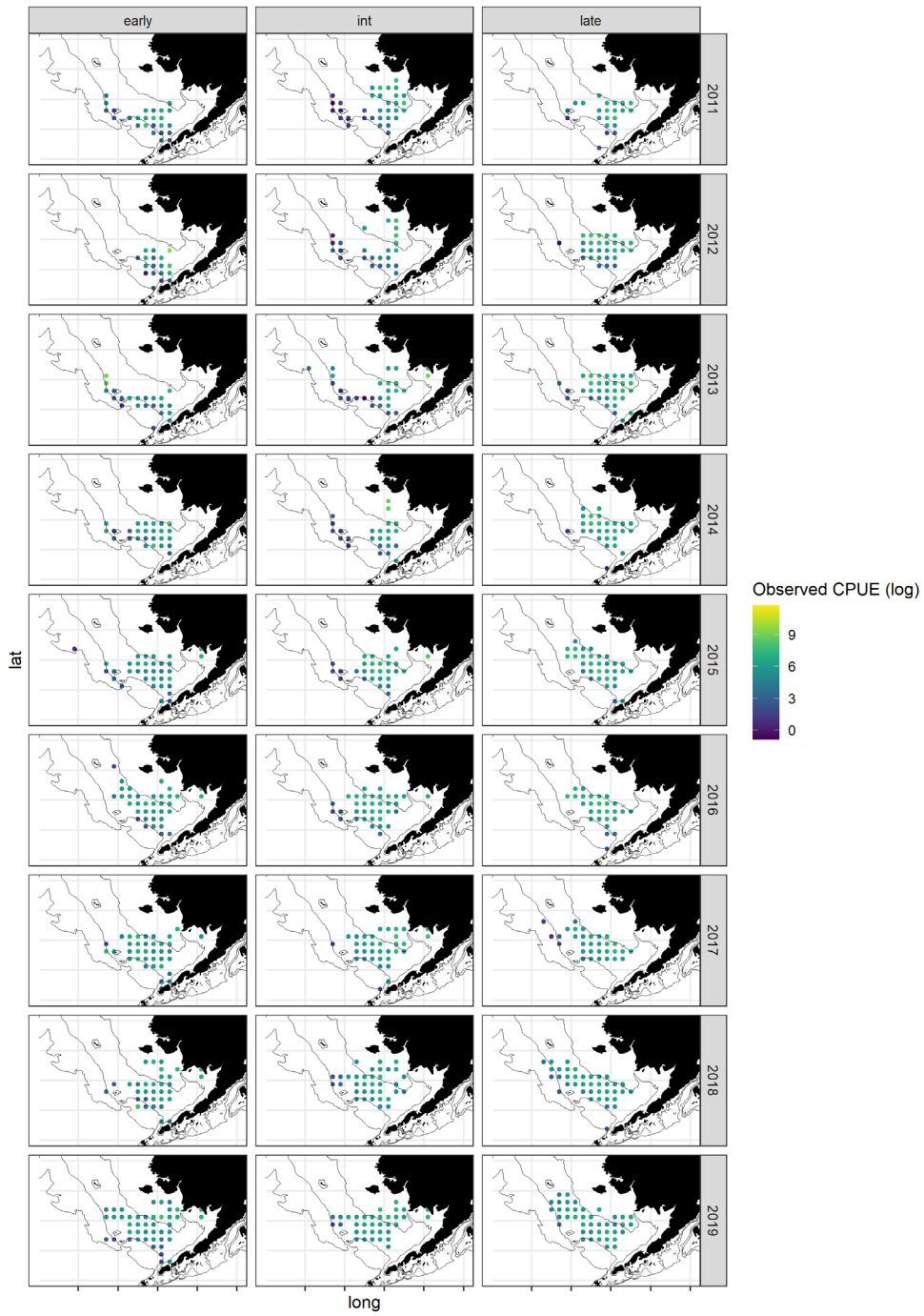


Figure S3: Spatiotemporal distributions of observed CPUE fisheries data

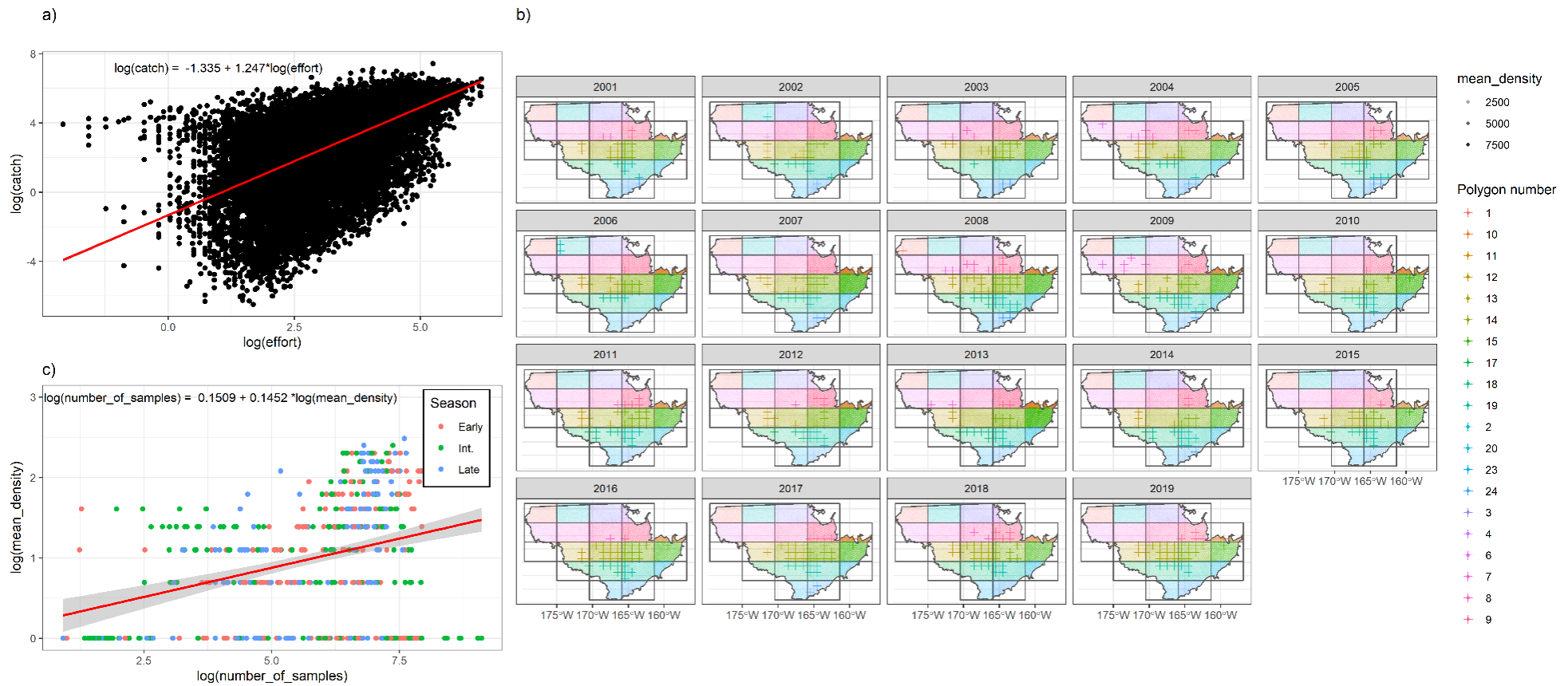


Figure S4: Diagnosis of any potential strong preferential sampling. a) Log-log plot between observed effort (sampling intensity) and observed catches. b) and c) aim at investigating any potential strong preferential sampling using predicted quantities by the model. b) For each season (here only intermediate season is represented), we divided the study area into a reduced number of 24 polygons (each polygon is associated with a specific color). Then for each season and year, we calculated the number of samples (represented by crosses) within each polygon and also we calculated the average predicted biomass within each polygon (low biomass are transparent and high biomass are plain colors). c) Log-log plot between number of samples and average biomass in each polygon for each season. A slope of 0.145 suggests a low sampling preference (based on Alglave et al. (2022))

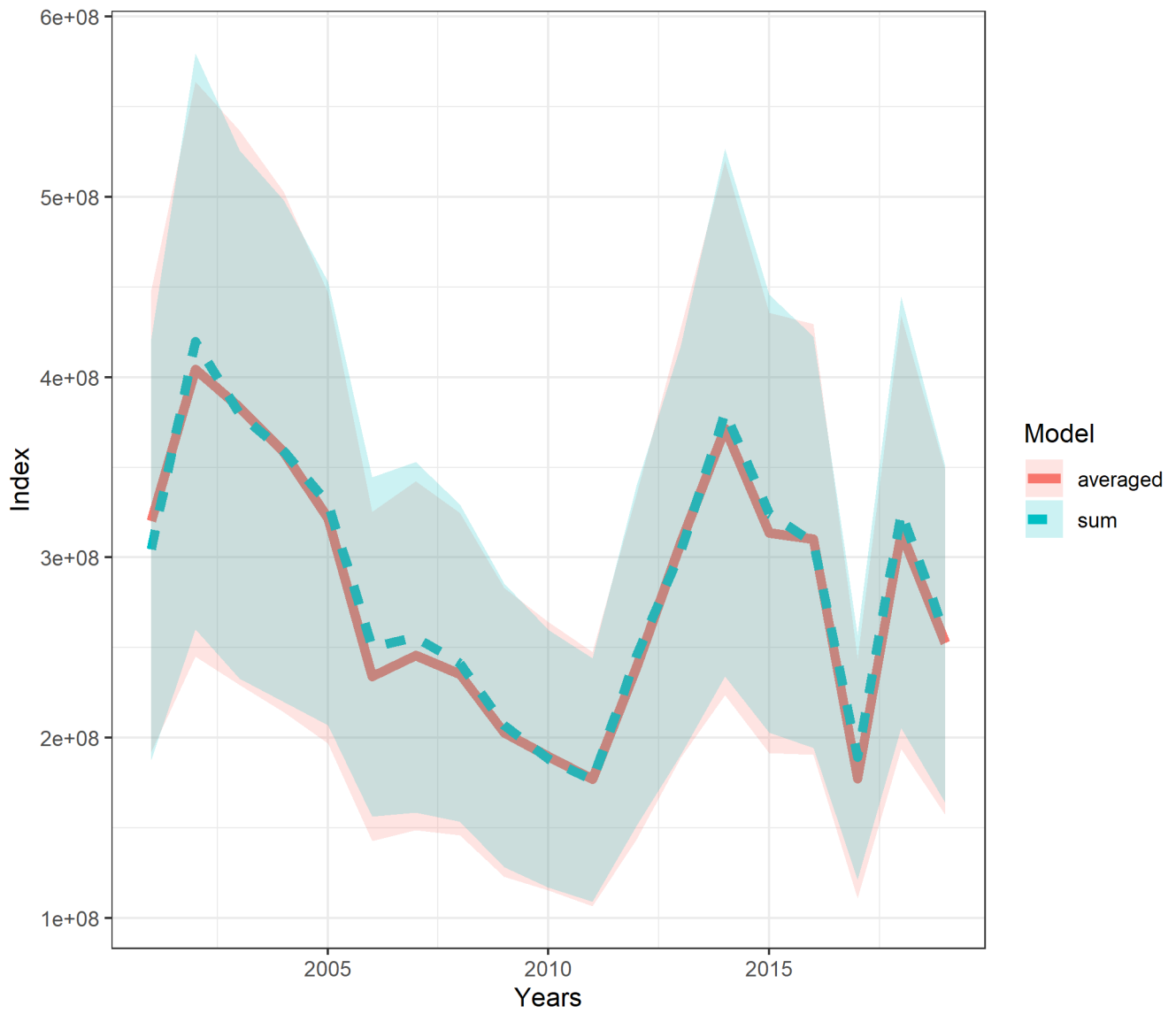


Figure S5: Comparison of index of biomass between models calculating CPUE as the ratio of the total catch in kg and the total effort within a ADFG cell (Model = sum) and as the ratio of catches in kg and effort averaged across ADFG (Model = averaged).

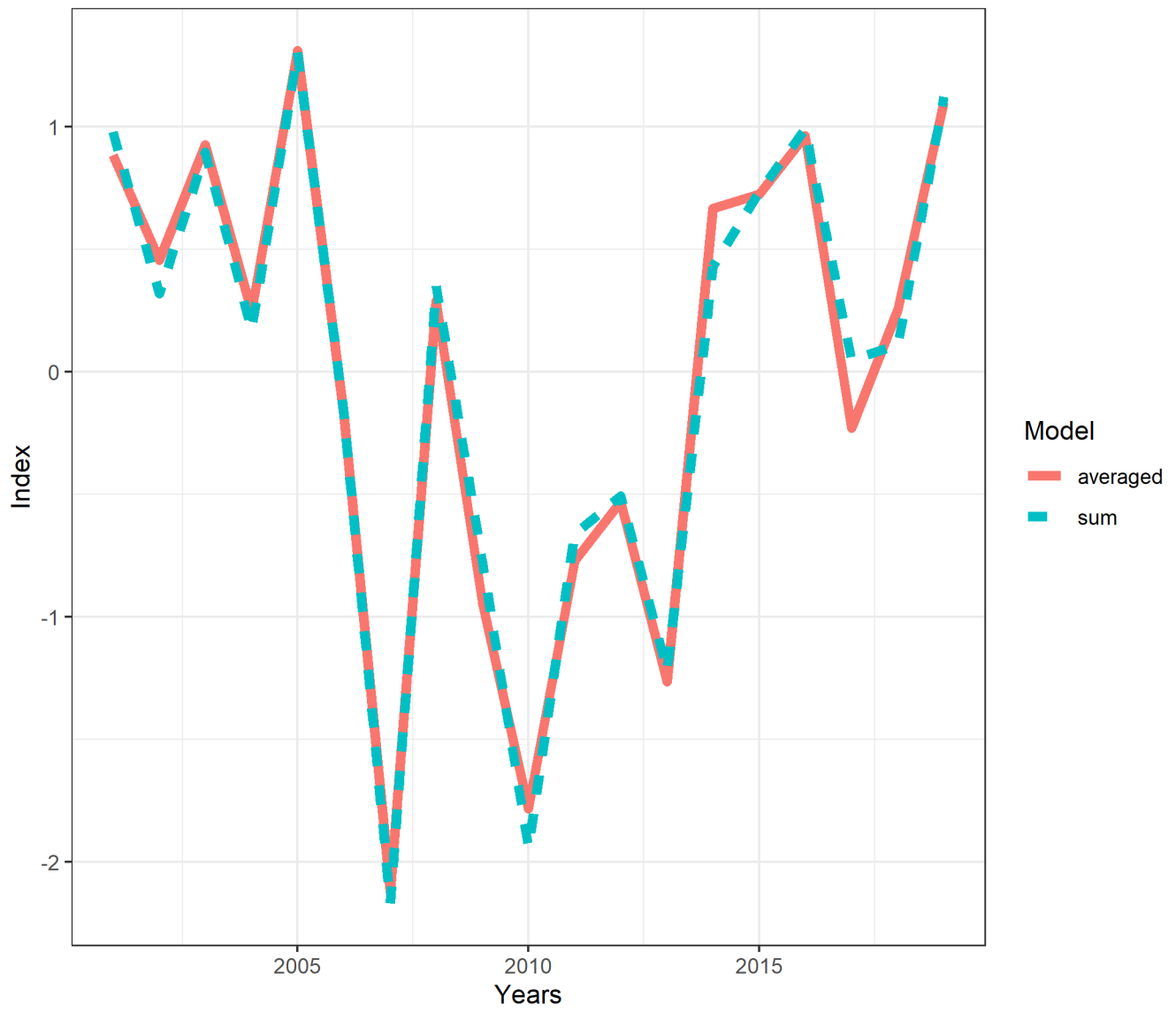


Figure S6: Comparison of overlap index of biomass between models calculating CPUE as the ratio of the total catch in kg and the total effort within a ADFG cell (Model = sum) and as the ratio of catches in kg and effort averaged across ADFG (Model = averaged).

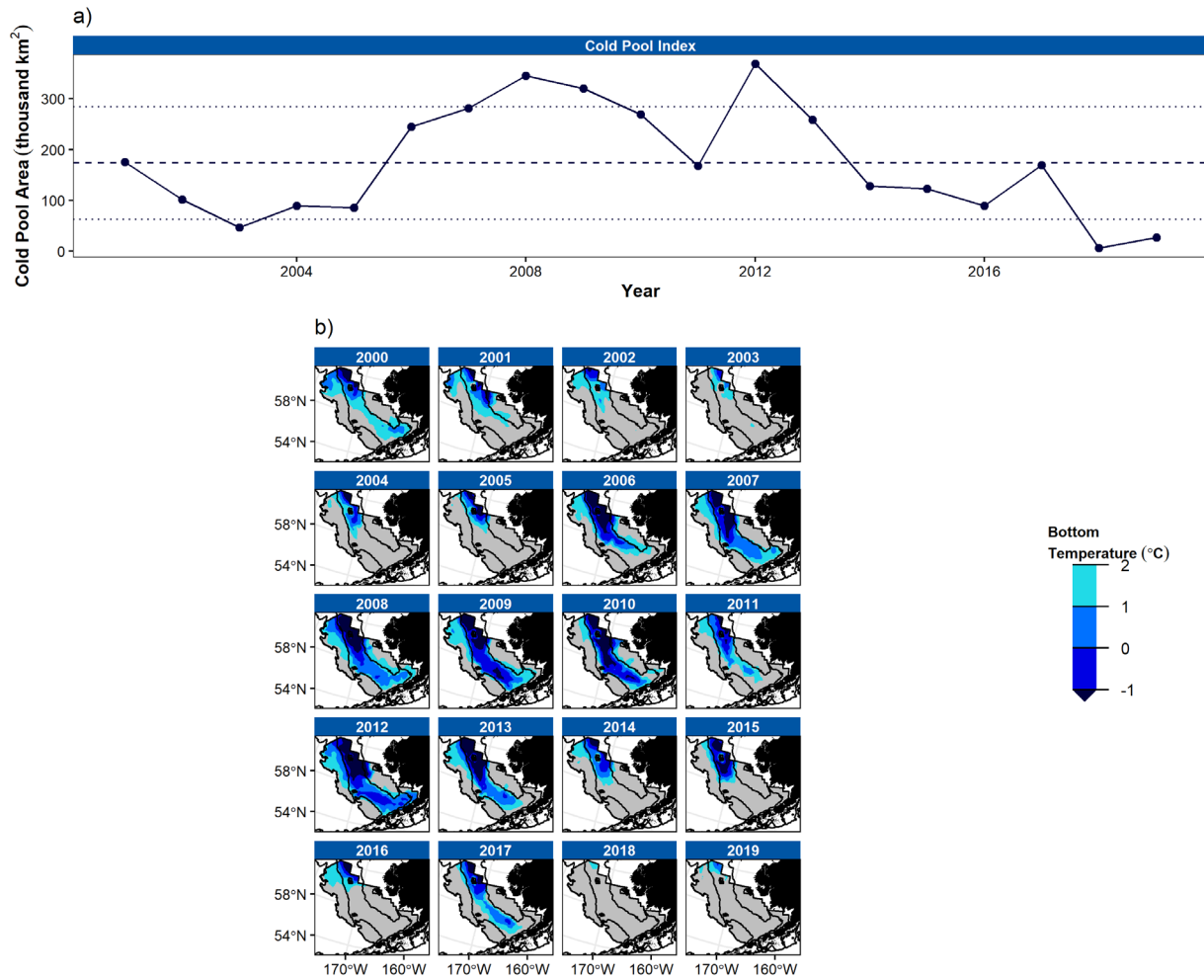
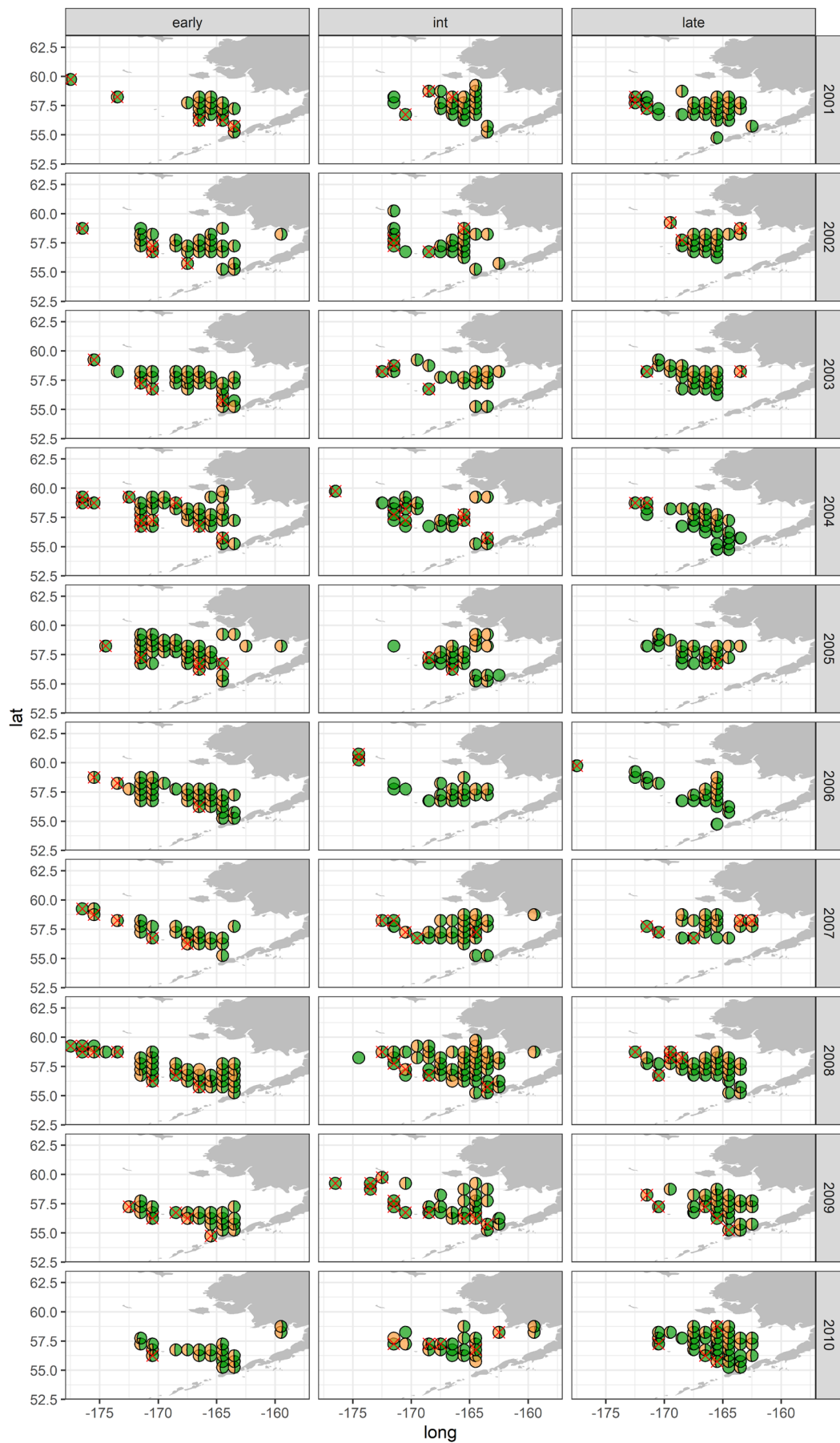


Figure S7: a) Standardized time series of cold pool extent (2001-2019). b) Spatial distribution of the cold pool (adapted from *akgfmmaps* package (<https://github.com/afsc-gap-products>)). According to Nichol et al., (2019) warm years are 2002,2003,2004,2005,2014,2015,2016 and cold years are 2006,2007,2008,2009,2010,2012,2013,2017. Years 2001, 2011 and 2017 are not particularly warm or cold (2018 and 2019 were not included in Nichol's study but can be defined as warm years). Because we did not want to define a supplementary level "Temperate" for the covariate *environmental conditions* (not enough data to have a balanced sampling with 3 levels for the covariate *environmental conditions*), we decided to define 2001 as a warm year and 2011 and 2017 as cold years. Indeed, yellowfin sole being a bottom fish, we considered that 2001 warmer than 2011 and 2017 because based on panel b) the extend of cold water (<1 C) is smaller for 2001 than for 2011 and 2017.



Sex
 ● F
 ● M

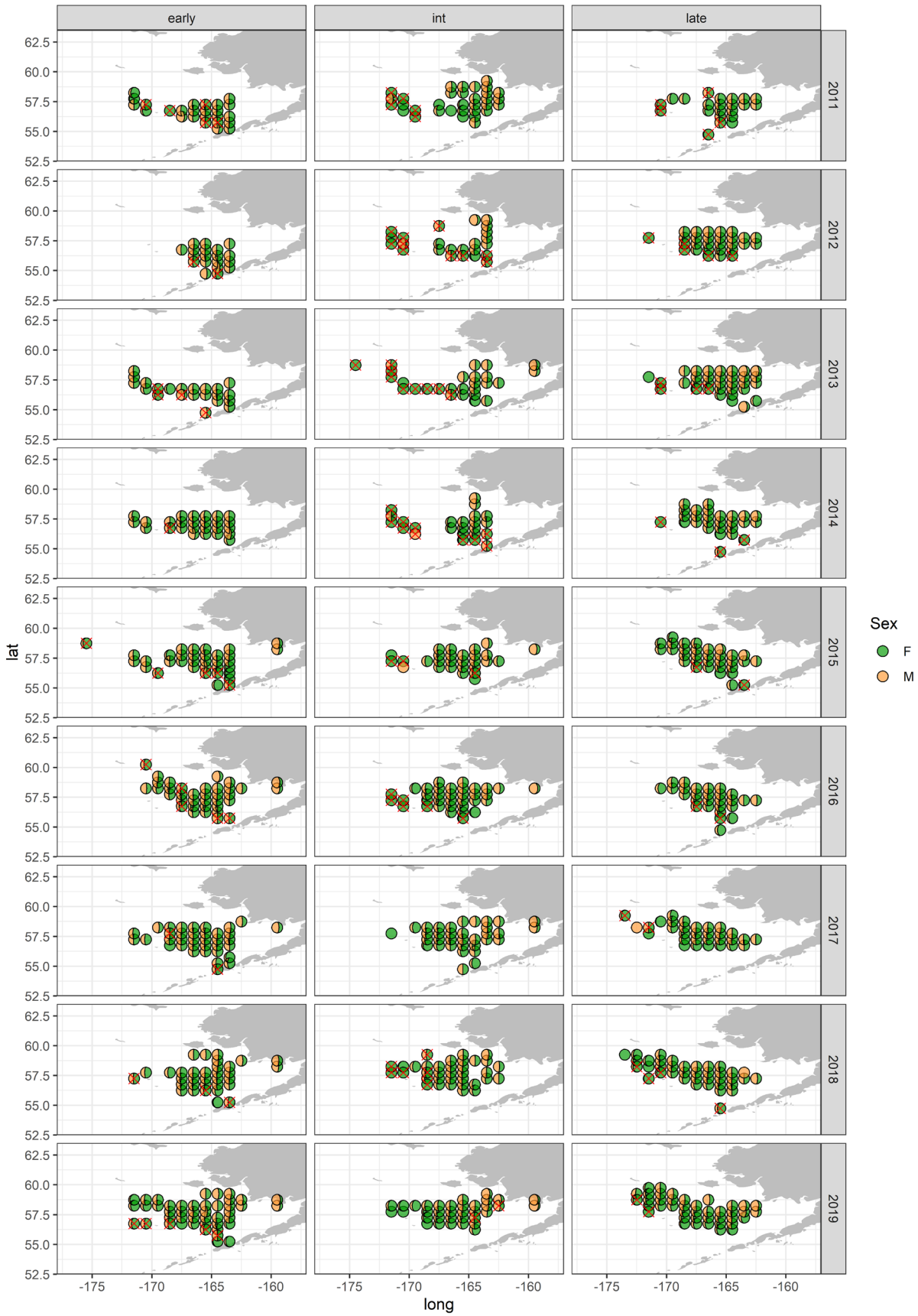


Figure S8: Spatiotemporal distribution of proportion of male and female CPUE (green=Female, orange=Male). Red cross represents locations where data were not available. We attributed to these locations the value of the closest neighbor for a given year and a given combination of covariates (i.e. all combinations of levels constituting seasons and environmental covariates)

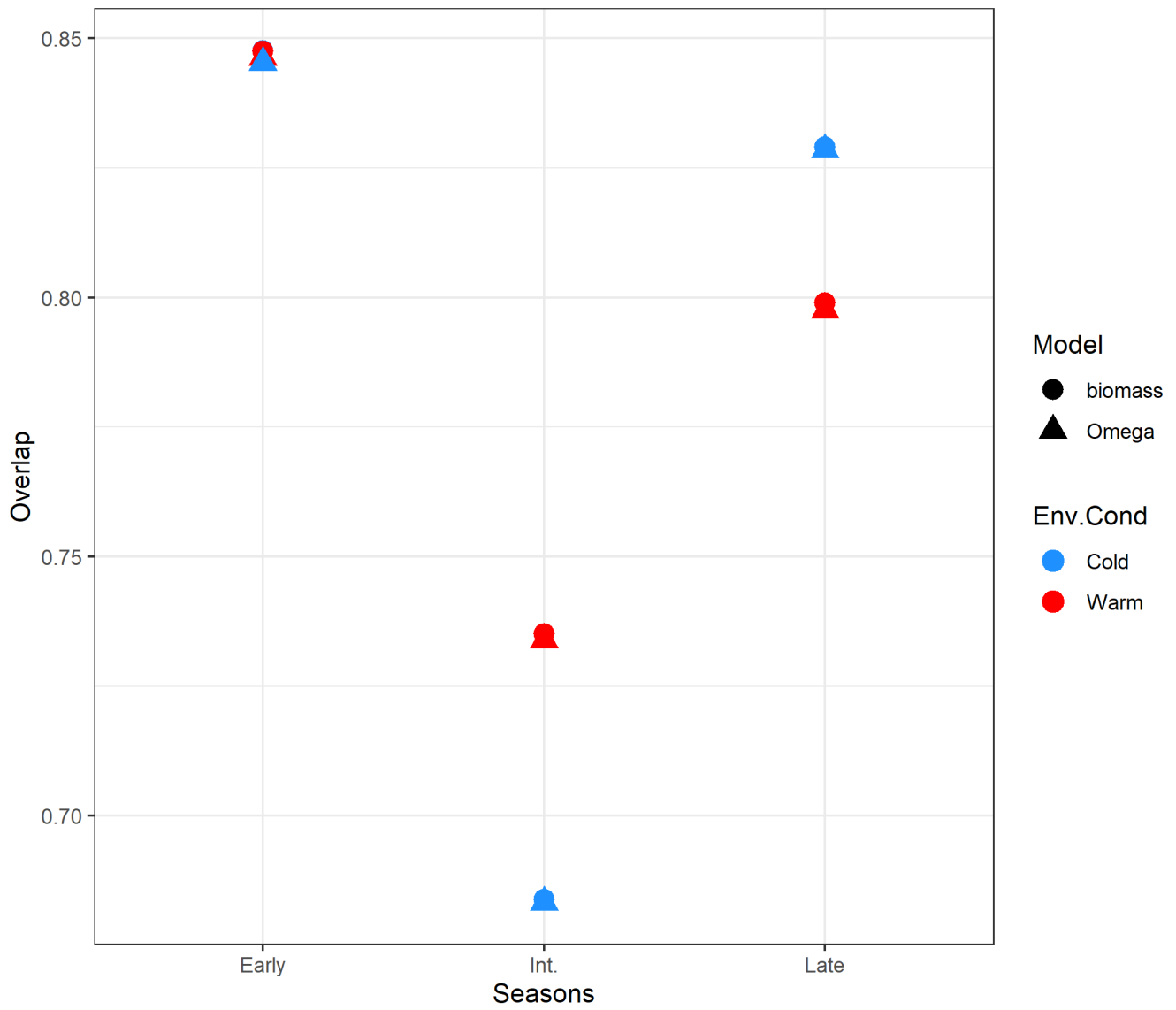


Figure S9: Comparison of averaged overlap among seasons and environmental conditions. Overlap was calculated from the predicted biomass (Model=biomass) or from the expected spatial main effect (model= Omega)

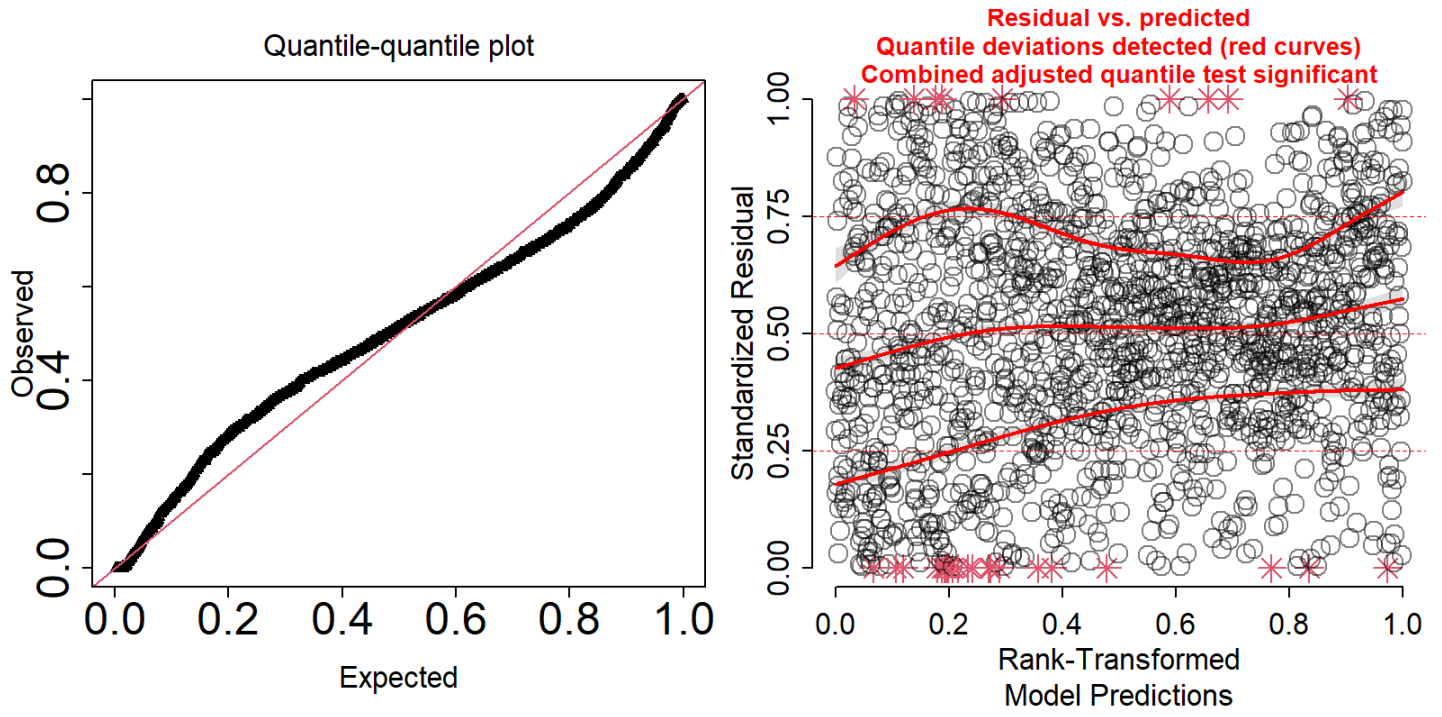


Figure S10 : Model diagnostics output showing the Q-Q plot residuals and how residuals vary with magnitude of the predictions.

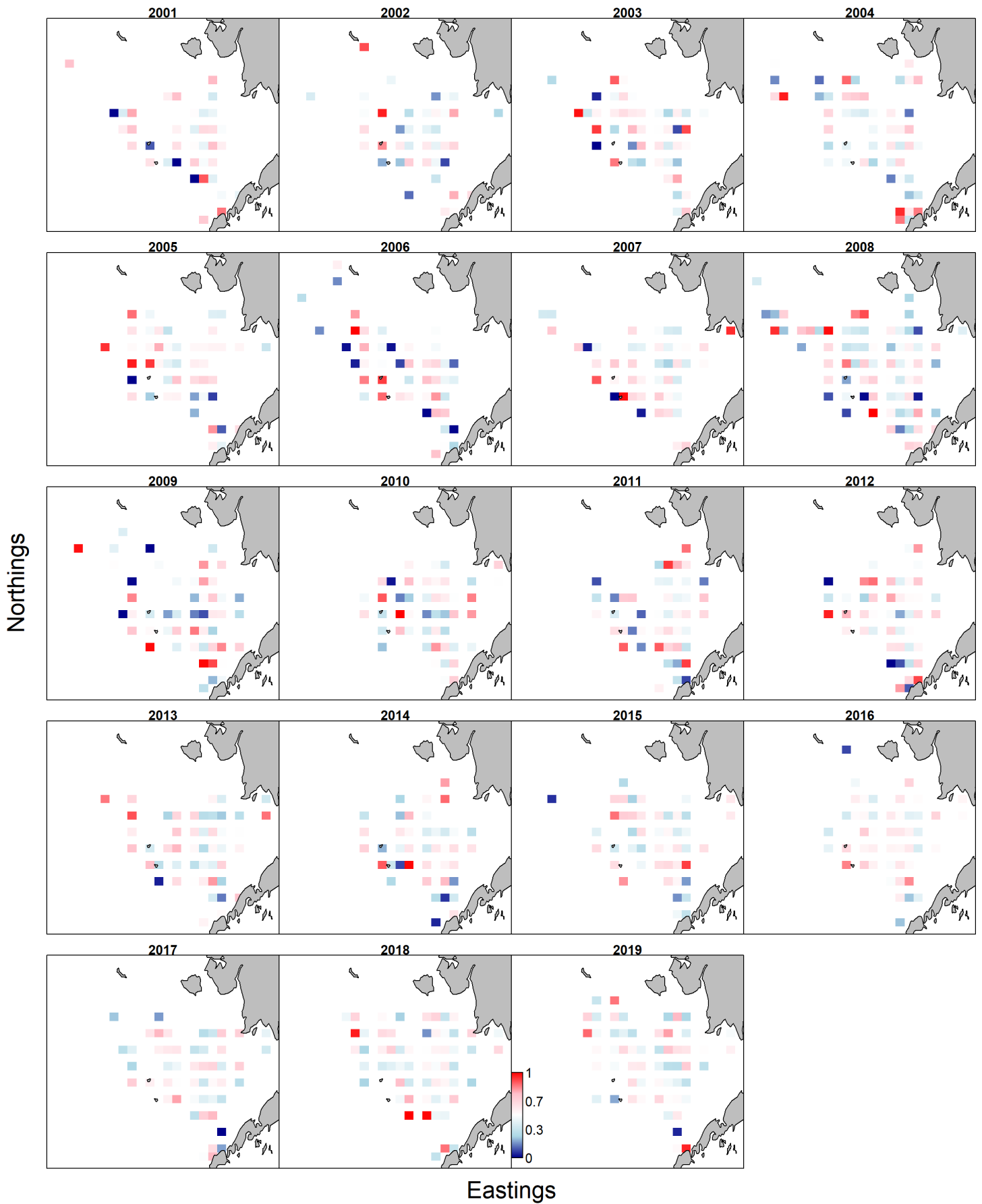
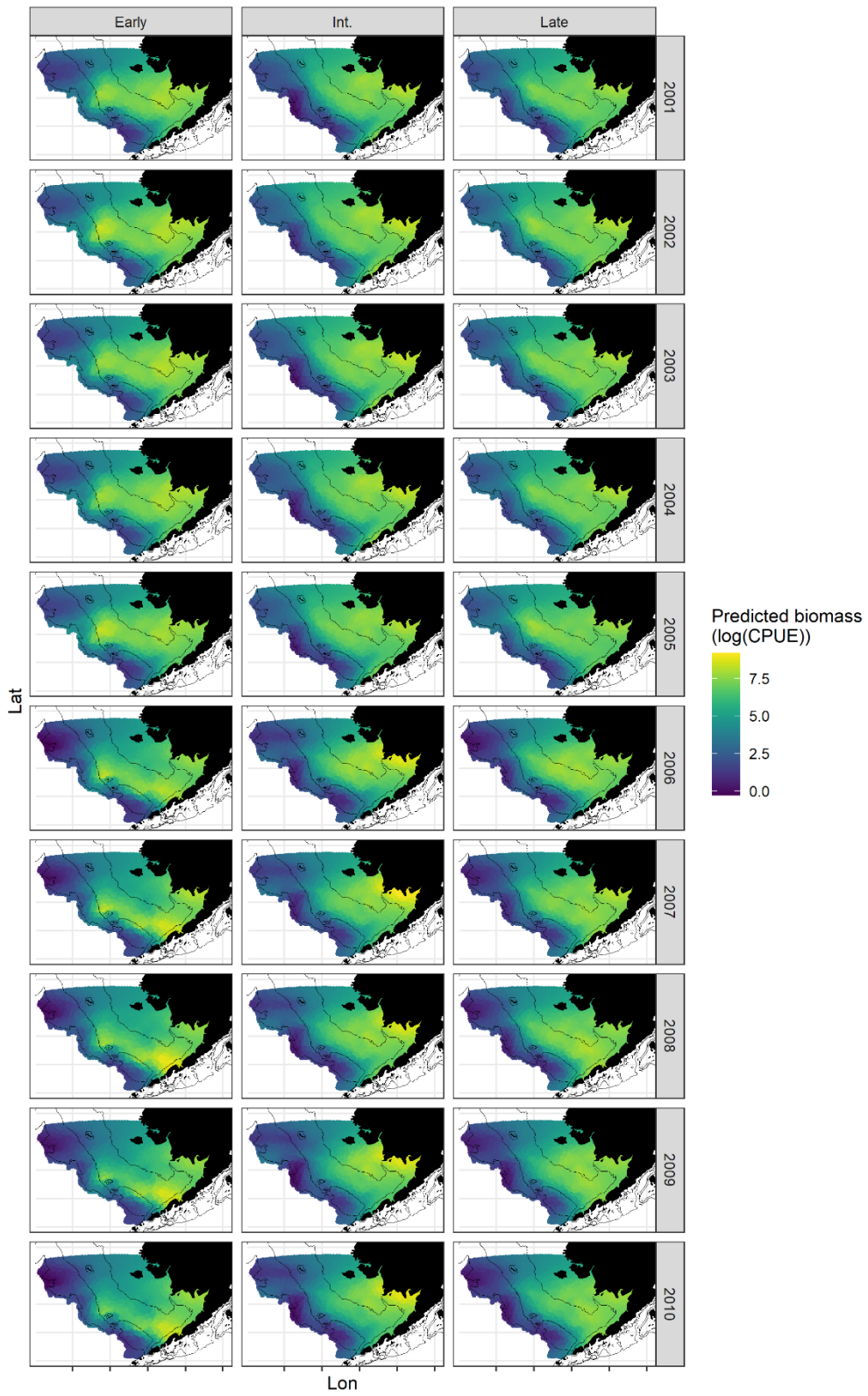


Figure S11 : Models diagnostics outputs showing spatial map of quantile residuals



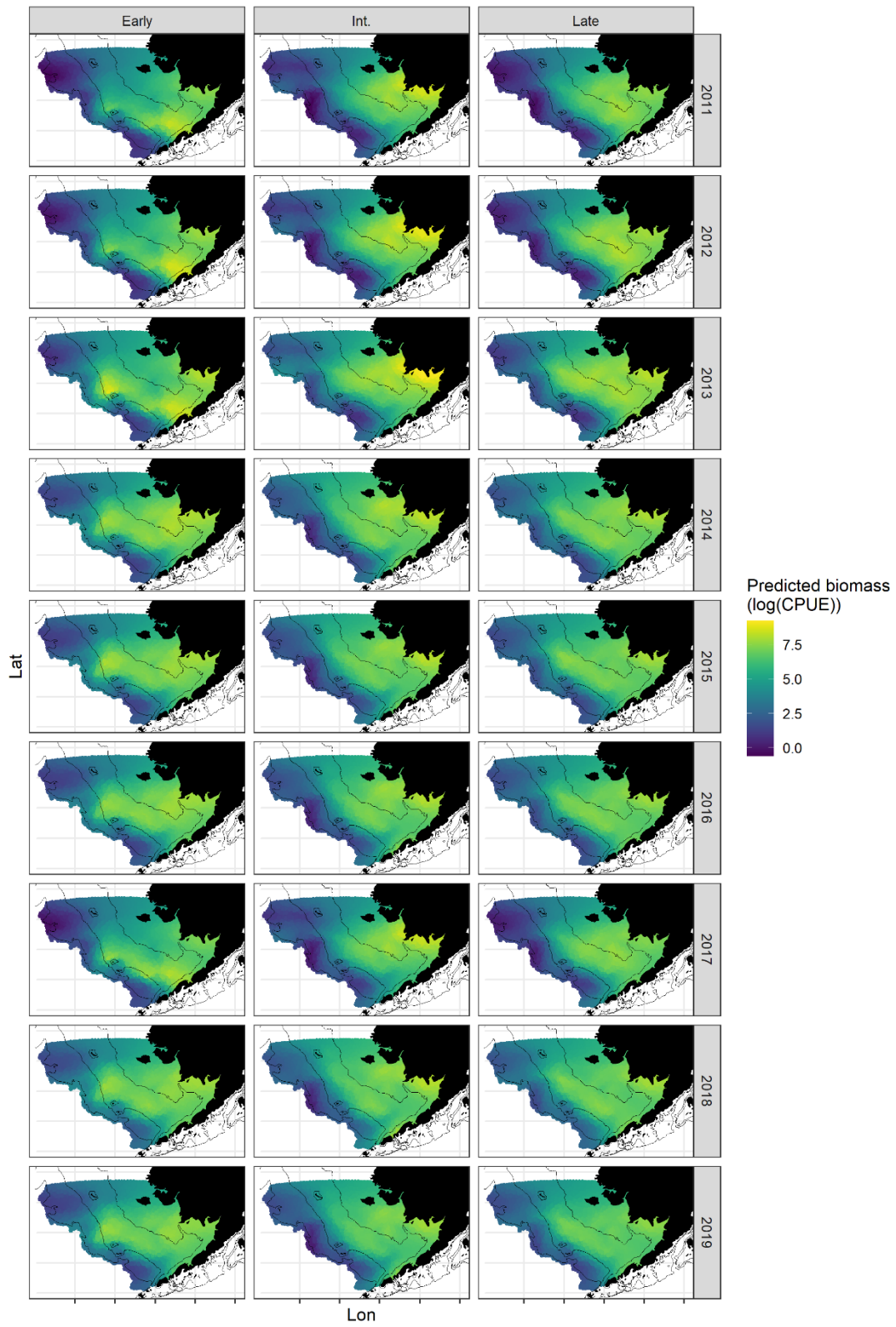


Figure S12: Seasonal spatiotemporal distribution of CPUE. Seasons are defined as Early, Intermediate (Int.) and late seasons.

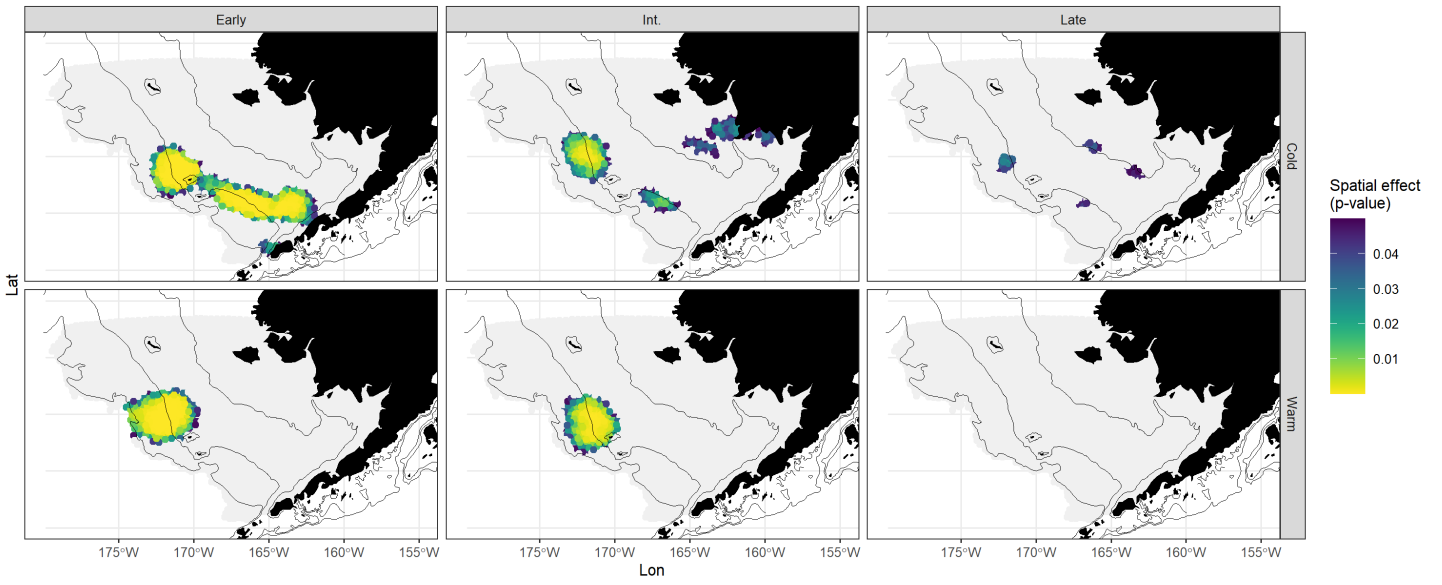


Figure S13: Significant effects of spatial variation covariate effects φ on fisheries CPUE

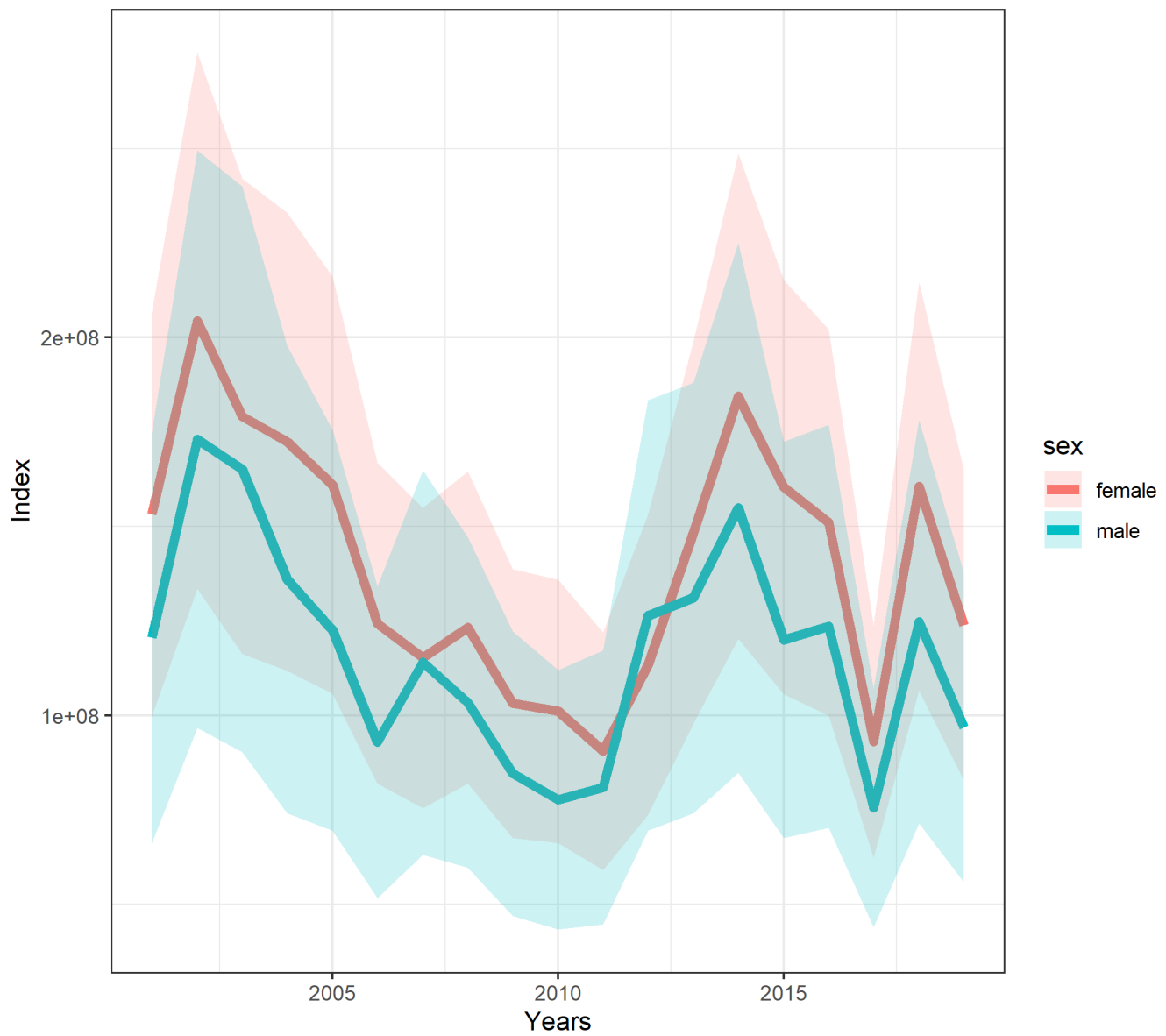


Figure S14: Time series of index of biomass for female and male yellowfin soles

S15: Comparing results using fishery dependent data to results from independent data

To justify that the ecological processes we are studying in this paper can be only inferred with fishery-dependent data and no fishery independent data, we also ran our analysis with fishery independent data as a sensitivity analysis.

Method

To this goal, we extended our approach by applying our model (Eq1.) to survey data for years 2001 to 2019. In particular, we represented the relationship among observed biomass (ratio of biomass and area swept) at time t_i at location s_i and the predicted positive local biomass (ratio of biomass and area swept) and the encounter probability using the widely used "Poisson-link" delta model (Thorson, 2018; Thorson & Barnett, 2017). We accounted for temperature effect only on the encounter probability because the goal of this study is to investigate how temperature affects movement phenology, i.e the presence of fish in a given area at a specific moment.

To sum up, in this new model:

- There is only one season (Intermediate Season, because no fishery independent data are available for the early and late seasons)
- We accounted for the effect of temperature (cold year vs warm years on survey CPUE) on biomass
- We used the same extrapolation grid (Fig.S1) that the one we used for the model with fishery dependent data. Using this extrapolation grid (that includes the fishery independent footprint and the area not available to the survey) we are able to show if the model with fishery independent data is able to infer the processes occurring outside the survey area.
- We finally re-generated Fig.5, Fig.6, and Fig.S13 to figure out if we can answer the questions addressed in this study.

Results

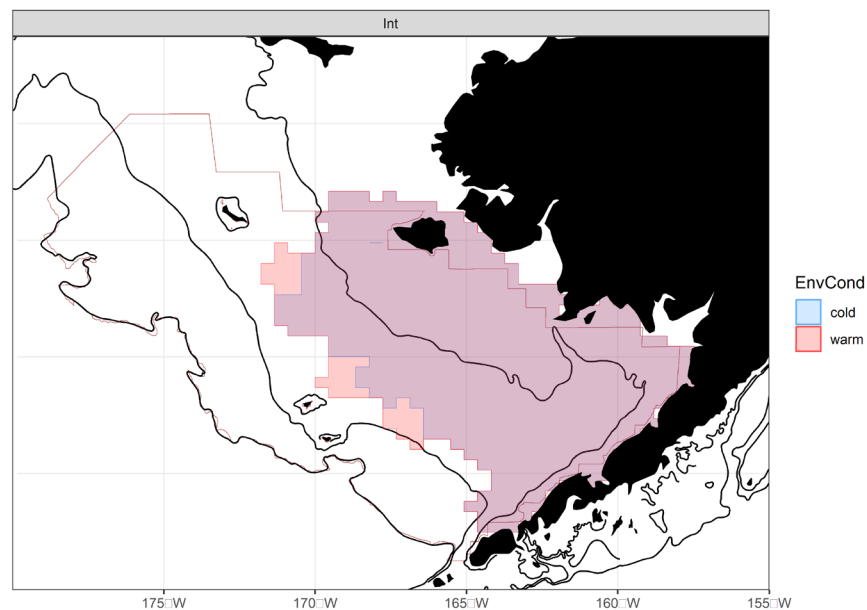


Figure S15.1: Spatial biomass distribution of yellowfin sole averaged for warm years (red) and cold years (blue). Red and blue polygons represent the cumulative biomass including 95% of the total biomass across the entire spatial area for warm and cold years respectively and for the Intermediate season (survey season). Brown polygon represents the survey area.

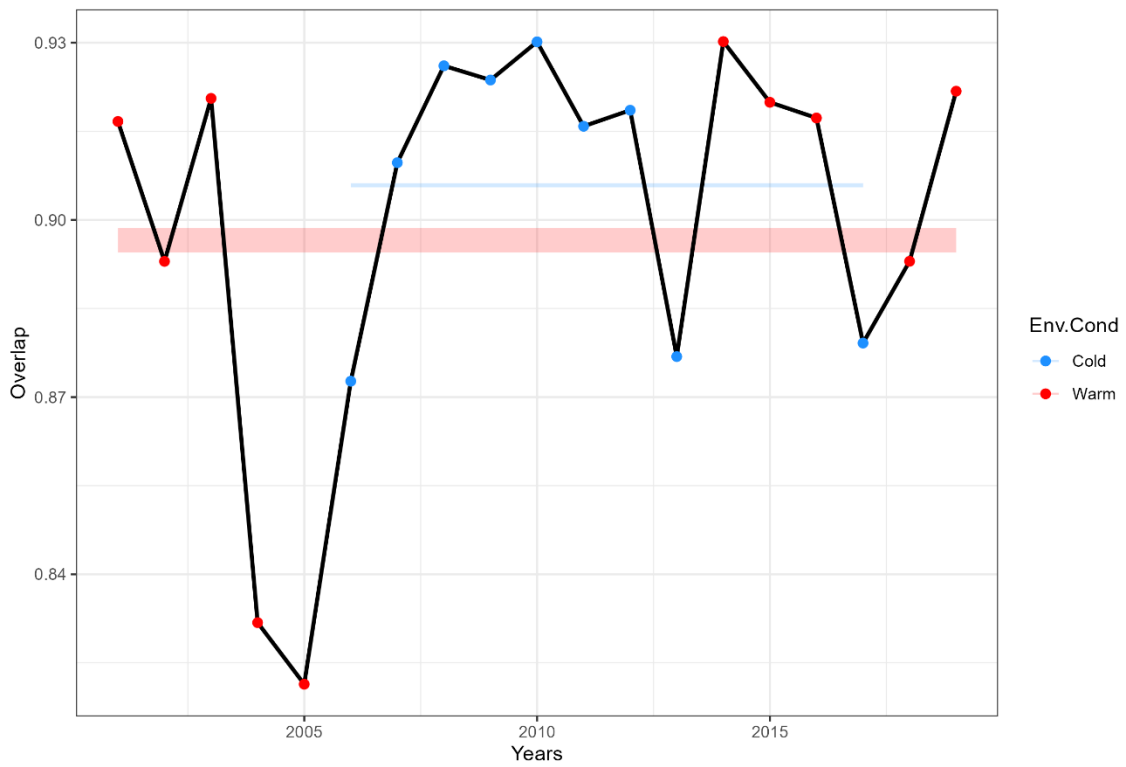


Figure S15.2 Time series of the overlap between spatial distribution of fishery CPUE biomass and survey spatial footprint during the intermediate season (survey season). Thick lines represent the averaged overlap across years (thickness of the line represent the standard deviation)

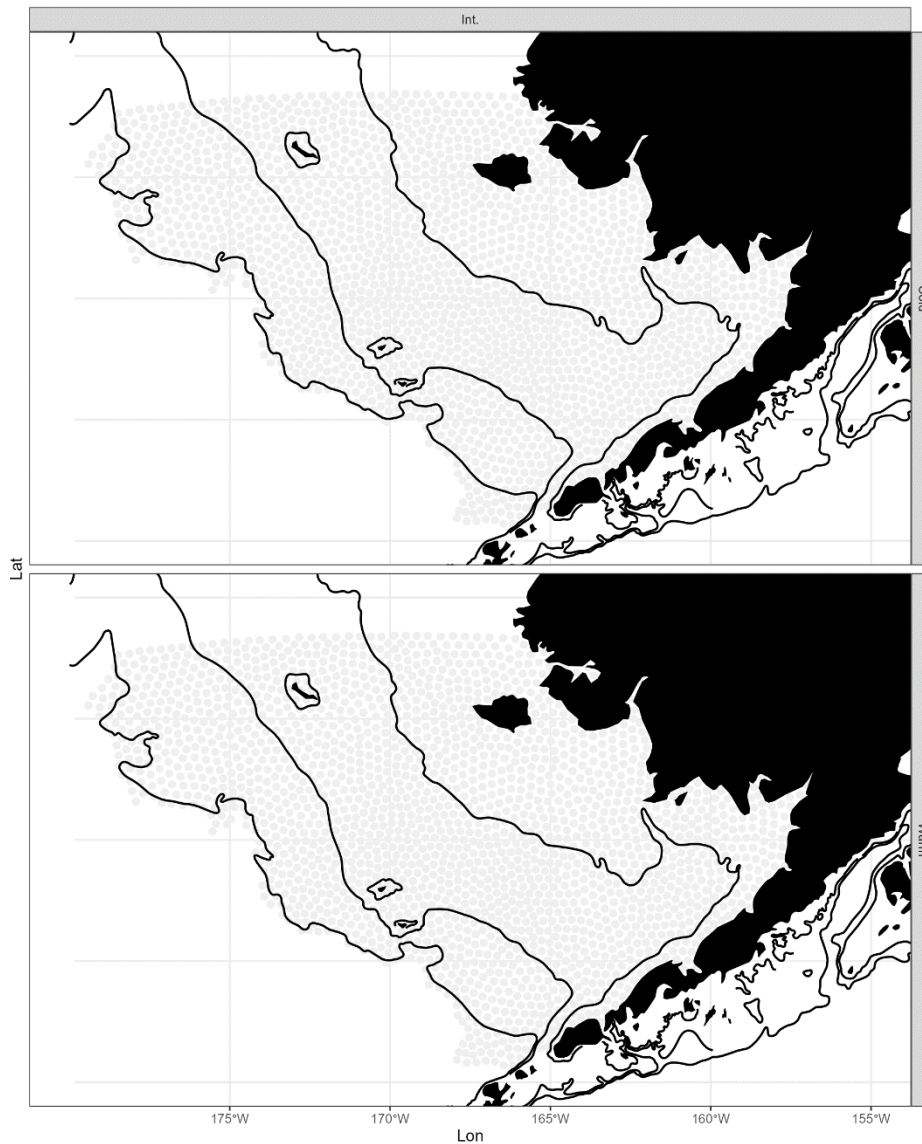


Figure S165.3: Significant effects of spatial variation covariate effects ϕ on survey data. Grey dots represent a non-significant effect.

First because survey data are only available during the intermediate season and are not defined across the all study area it is very difficult to infer changes in movement phenology based on those data. Then, this present sensitivity analysis justifies that the ecological processes we are investigating in this study can be only inferred with fishery-dependent data and no fishery independent data, and this because of three main reasons:

1. When using survey data, there is small differences in distributions of survey data between cold and warm years. In warm years the distributions of survey data are more spread out over the middle shelf (Fig S15.1). However, the model cannot predict any differences on the inner shelf (Fig S15.1), unlike the model using fishery data (Fig. 5).
2. Additionally, the model using survey data cannot infer any significant effect between temperature changes and survey biomass (Figure S15.3).
3. Predicting the survey biomass outside the survey area using VAST (i.e, autocorrelated function) did not provide any insight about the presence of fish outside the survey area (Fig. S15.2) because of the higher predictive uncertainty when predicting density in areas with zero observed data (Fig. S15.2).